NOTICE

AVIS

The quality of this microform is heavily dependent upon the quality of the original thesis submitted for microfilming. Every effort has been made to ensure the highest quality of reproduction possible.

La qualité de cette microforme dépend grandement de la qualité de la thèse soumise au microfilmage. Nous avons tout fait pour assurer une qualité supérieure de reproduction.

If pages are missing, contact the university which granted the degree.

S'il manque des pages, veuillez communiquer avec l'université qui a conféré le grade.

Some pages may have indistinct print especially if the original pages were typed with a poor typewriter ribbon or if the university sent us an inferior photocopy.

La qualité d'impression de certaines pages peut laisser à désirer, surtout si les pages originales ont été dactylographiées à l'aide d'un ruban usé ou si l'université nous a fait parvenir une photocopie de qualité inférieure.

Reproduction in full or in part of this microform is governed by the Canadian Copyright Act, R.S.C. 1970, c. C-30, and subsequent amendments.

La reproduction, même partielle, de cette microforme est soumise à la Loi canadienne sur le droit d'auteur, SRC 1970, c. C-30, et ses amendements subséquents.

Canada

UNIVERSITY OF ALBERTA

THE EFFECT OF AIR FLOW ON HEAT TRANSFER THROUGH POROUS INSULATION

BY

MOURAD CHEKHAR

A thesis submitted to the Faculty of Graduate Studies and Research in partial fulfilment of the requirements for the degree of Master of Science

DEPARTMENT OF MECHANICAL ENGINEERING

EDMONTON, ALBERTA
AUGUST,1995

ISBN   0-612-06455-7

Canada

UNIVERSITY OF ALBERTA

RELEASE FORM

AUTHOR   :   Mourad Chekhar

TITLE   :   THE EFFECT OF AIR FLOW ON HEAT TRANSFER THROUGH POROUS INSULATION

DEGREE   :   Master of Science

GRANTED   :   August, 1995
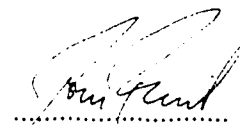
#301,10842-107 Street

Edmonton, Alberta

T5H 2Z3

CANADA
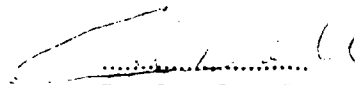
August 31st, 1995

UNIVERSITY OF ALBERTA

FACULTY OF GRADUATE STUDIES AND RESEARCH
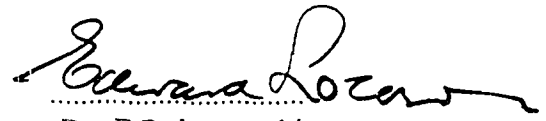
THE UNDERSIGNED CERTIFY THAT THEY HAVE READ, AND RECOMMENDED TO THE FACULTY OF GRADUATE STUDIES AND RESEARCH FOR ACCEPTANCE, A THESIS ENTITLED THE EFFECT OF AIR FLOW ON HEAT TRANSFER THROUGH POROUS INSULATION SUBMITTED BY MOURAD CHEKHAR IN PARTIAL FULFILMENT OF THE REQUIREMENTS FOR THE DEGREE OF MASTER OF SCIENCE

....
Dr. T.W. Forest
(Supervisor)

....
Dr. J.D. DALE

....
Dr. E.P. Lozowski

August 24ᵗʰ, 1995

TO THE DREAMERS

ABSTRACT

An experimental study was conducted to investigate systematically the effect of air flow over an exposed surface on heat transfer through porous insulation. Tests were carried out in a small, non-recirculating wind tunnel with standard thickness insulation sample of 89 mm mounted flush with the floor of the tunnel. Temperature distributions and heat fluxes were measured at several locations with each sample for a range of tunnel velocities from 0 to 9 m/s. Glass fibre based porous insulation was tested for a range of permeabilities of 2×10^{-8} m^2 to 5×10^{-9} m^2, the latter limit corresponding to commercial glass fibre insulation.

Experimental results indicate that the mean heat flux increases significantly with increasing air flow velocity over the exposed surface of the insulation. This is a direct result of air intrusion into the porous insulation. Effective thermal resistance values were decreased by a factor of 2 to 3 for velocities up to 7 m/s. For the highest permeability sample (lowest density) tested, the zero velocity R-value is approximately twice the value of commercial glass fibre insulation but is much more sensitive to the effects of air flow. For a range of velocities from 0 to 9 m/s, the R-value decreases from 4 to 2 .

This study showed that heat transfer through porous insulation can be increased significantly by air flow over an exposed surface of the sample. This has implications for the use of this type of insulation in certain areas of building envelopes.

ACKNOWLEDGEMENTS

CONTENTS

LIST OF FIGURES

LIST OF TABLES

NOMENCLATURE

A : Cross section area of the sample (m^2)

c_p : Specific heat at constant pressure for air (J/kg.K)

d : Width of the insulation sample (mm)

g : Gravitational acceleration (m/s^2)

K : Permeability of porous medium (m^2)

P : Pressure (N/m^2)

k : Thermal conductivity of porous medium (W/m.K)

q : Specific heat flux (W/m^2)

Q : Volume flow rate (m^3/s)

T_c : Temperature of the upper surface of the sample (°C)

T_w : Temperature of the bottom surface of the sample (°C)

T_e : Temperature at the entrance of the sample (°C)

ΔT : Temperature difference between the warm side and the cold side (°C)

u : Velocity in the x-direction (m/s)

u_f : Velocity of the free steam (m/s)

u_m : Air flow velocity in the porous insulation sample (m/s)

v : Velocity in the y-direction (m/s)

w : Velocity in the z-direction (m/s)

x : Horizontal position coordinates measured from the entrance edge of the sample (mm)

y : Lateral position (depth) measured from the side of the sample (m)

z : Vertical position (Height) measured from the bottom of the sample (m)

Da : Darcy number

Nu : Nusselt number

Ra : Rayleigh number

Re : Reynolds number

V_S : Solid volume of porous insulation (m^3)

V_T : Total volume of porous insulation (m^3)

GREEK SYMBOLS

α : Thermal diffusivity of fluid-saturated porous media (m^2/s)

β : Coefficient of thermal expansion (K^{-1})

ρ : Density (kg/m^3)

ρ_a : Density of air (kg/m^3)

ρ_s : Density of solid matrix material of the porous media (kg/m^3)

γ : Dimensionless constant

μ : Dynamic viscosity (kg/m.s)

ν : Kinematic viscosity (m^2/s)

Φ : Density of porous insulation

INTRODUCTION

Porous media are encountered in a broad range of engineering problems associated with such diverse areas as ground water hydrology, oil and gas reservoirs, and the use of porous media as insulation. Porous insulation may have an open-pore configuration consisting of glass fibres, wood fibres or granular materials. In this type of insulation the pore spaces are interconnected and open to the surrounding air at its surface. Other types of insulation such as foam rigid board have isolated pockets which are not interconnected. It is the low thermal conductivity of the trapped air that gives insulation its high resistance to heat flow. The thermal performance of insulation is largely governed by its ability to prevent air movement within its structure.

In some applications, open-pore insulation such as glass fibre batt may be subject to air flow parallel to one surface of the batt. In houses, such cases occur in cathedral ceilings where the roof insulation has air flowing over the upper cold side of the insulation in a small air gap between the roof sheathing and the insulation; this ventilation air flow is required to remove moisture on the sheathing and prevent over-heating of the sheathing, (Fig.1.1). A similar case is encountered in flat-ceiling houses where the open-faced permeable insulation in the attic may be subject to ventilation air flow, (Fig.1.2). In either case, air flow over a free surface of porous insulation may induce some air motion within the insulation. If this occurs, then this convective air motion will alter the temperature profiles within the insulation producing a change in the heat flux.

A survey of the literature revealed that some work has been done on related problems but no systematic study has been conducted to quantify this effect. The first attempt to study the boundary conditions at an open permeable wall was made by Beavers and Joseph (1969). They described experiments which were designed to examine the nature of the tangential flow in the boundary region of a permeable interface. The

Porous medium

Air flow
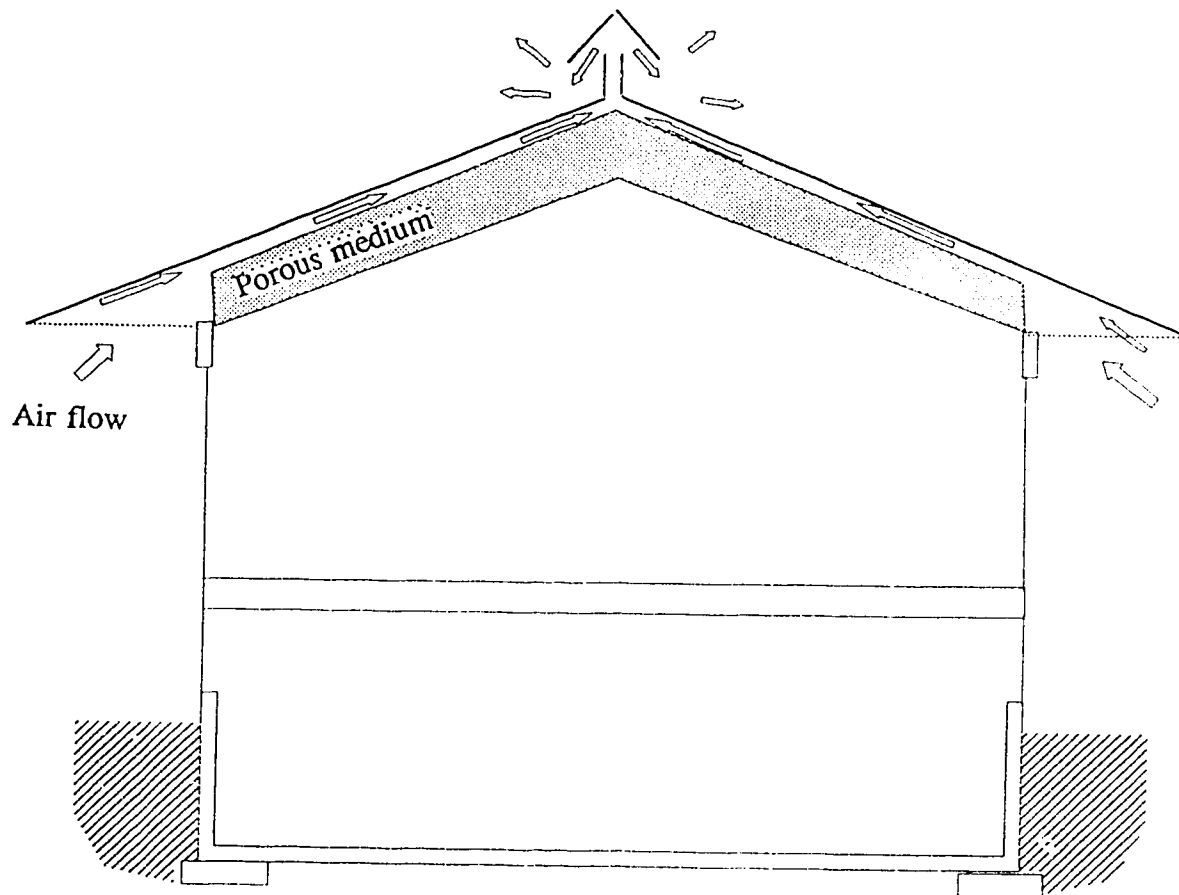
Figure 1.1 *House with a cathedral ceiling.*
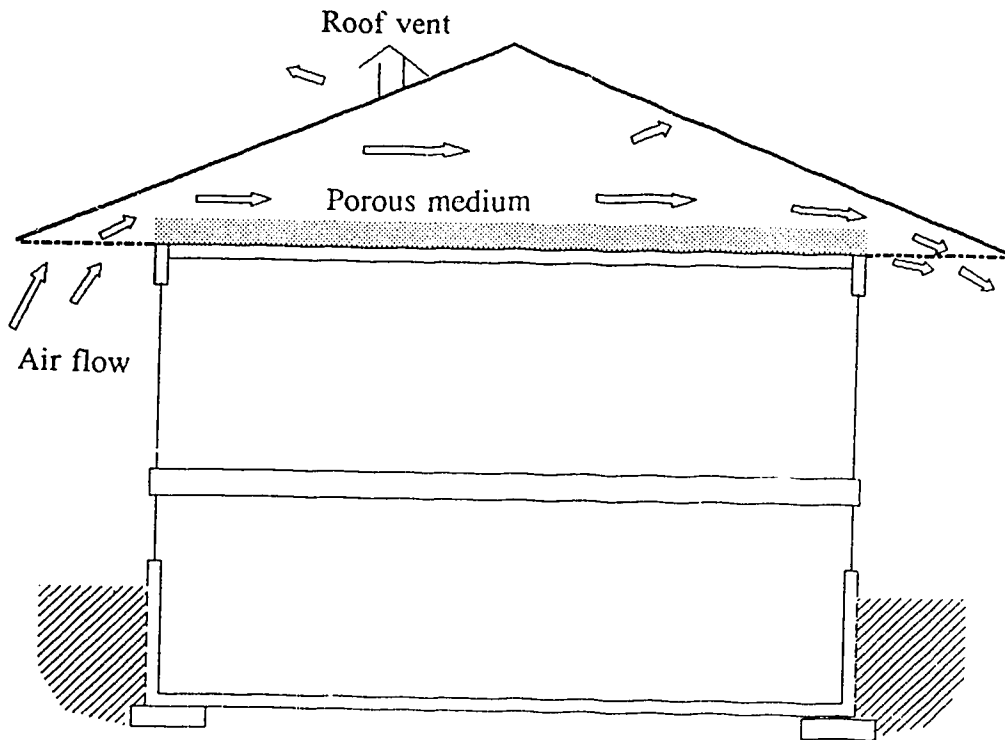
Figure 1.2 *House with flat ceiling.*

experimental arrangement consisted of flow through a long porous block and flow through a small uniform gap immediately above thisblock. The porous block was inserted into an open rectangular channel which connected an upstream reservoir with two downstream reservoirs. This arrangement was modeled as flow in which the Navier-Stokes equations were satisfied in the free fluid, Darcy flow was satisfied in the interior of the permeable material but not necessarily in the boundary regions, and the normal component of the velocity and the pressure were continuous at the porous boundary. The tangential component of velocity presumably changes across this layer from its statistically averaged Darcy value to some slip value immediately outside the permeable block. A simple theory based on replacing the effect of the boundary layer with a slip velocity proportional to the exterior velocity gradient is proposed and shown to be in reasonable agreement with experimental results. The result of the experiment indicated that the effect of viscous shear appeared to penetrate into the permeable material in a boundary layer region, producing a velocity distribution similar to that depicted in Fig 1.3. The tangential component of velocity of the free fluid at the porous boundary could be considerably greater than the mean filter velocity within the body of the porous material. This boundary layer could alter the nature of the tangential motion near the nominal boundary.
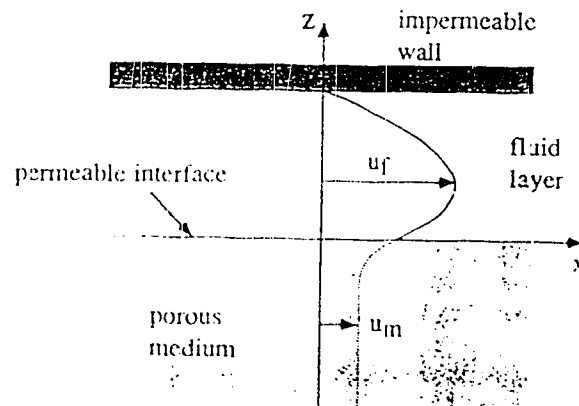
Figure 1.3 Velocity profile for unidirectional flow in a horizontal channel bounded by an impermeable upper wall and a saturated porous medium.

4

This work was soon followed by Saffman (1971), who used a theoretical justification for the empirical boundary condition proposed by Beavers and Joseph (1969), Eqn 1.1. He used a statistical approach to extend Darcy's law to non- homogeneous porous medium. The problem was regarded as a special case of flow through a non-homogeneous porous medium with the porosity and permeability changing from the value of unity and infinity to the values for the porous medium forming the boundary. The boundary condition, Eqn.1.1, could then be deduced by the application of standard boundary layer techniques to the equations describing flow through non-homogeneous media.

$$\frac{\partial u}{\partial n} = \frac{\gamma}{K^{1/2}}(u_f - u_m)$$

1.1

where u_f is the velocity in the fluid, u_m is the mean filter velocity (flux per unit area) in the porous medium, K is the permeability of the porous medium and γ is a dimensionless quantity independent of the viscosity of the fluid and dependent on the material parameters that characterize the structure of the permeable material within the boundary region.

Berlad *et al.* (1980) have examined the applicability of the classical thermal resistance or R-values to commonly encountered insulation systems where air intrusion is physically possible. One set of experimental apparatus (Fig.1.4) was employed to examine the existence-nonexistence of free convection effects within the body of a permeable insulation system. In this experiment, a sealed permeable glass fibre batt was vertically situated between parallel warm and cold boundaries. Extensive thermocouple arrays were employed to determine the horizontal temperature profiles within the body of glass fibre batt at three different heights. Temperature profiles shown in Figs 1.5 and 1.6 were obtained for a total temperature difference of 33.3°C and 73.9°C respectively. In each case the dashed (straight) line corresponds to the pure conduction case. The solid curve was drawn through the temperature data for the three planes. A second apparatus (Fig.1.7) was employed to examine the effect of intrusion on a specimen of permeable insulator. Three cases corresponding to an insulator heated from below, and open to room
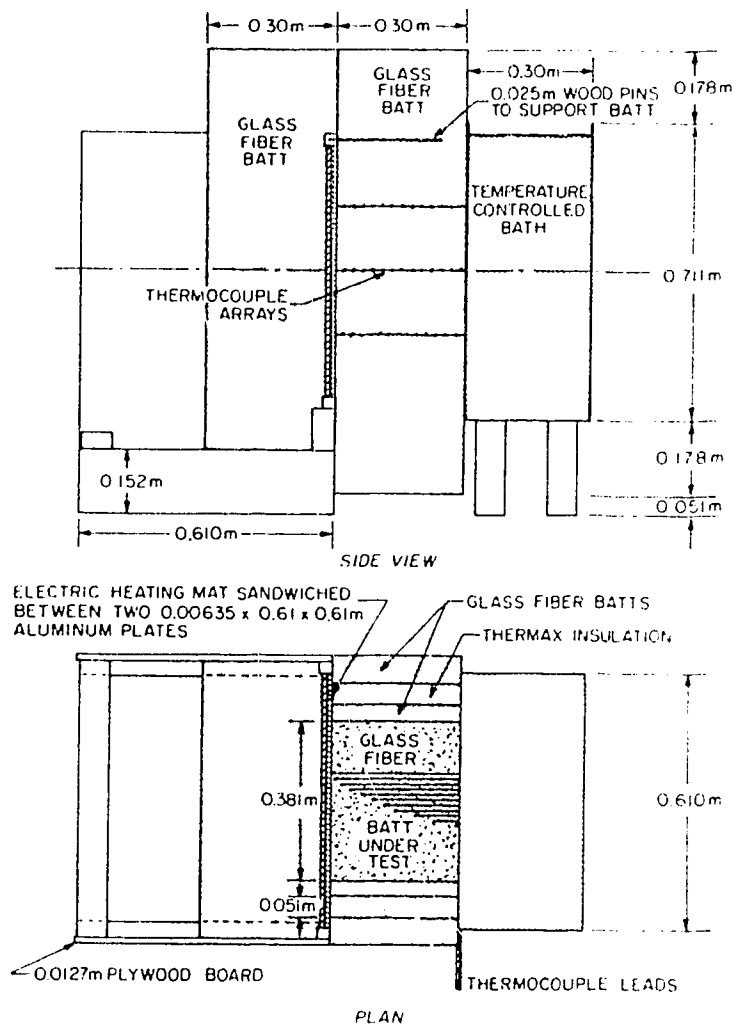
Figure 1.4 *Glass fibre batt heated along a vertical surface.*

6
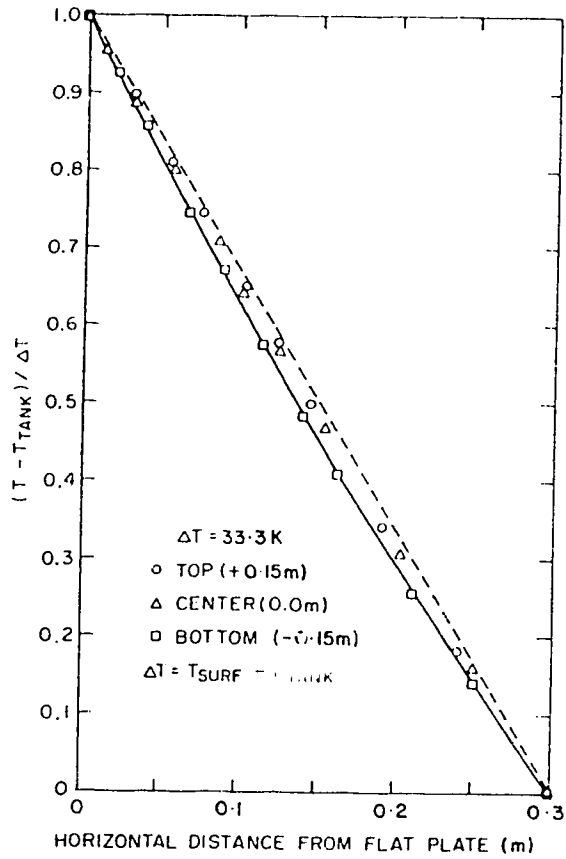
Figure 1.5 *Horizontal temperature profiles in a vertically situated glass fibre batt (ΔT= 33.3°C).*
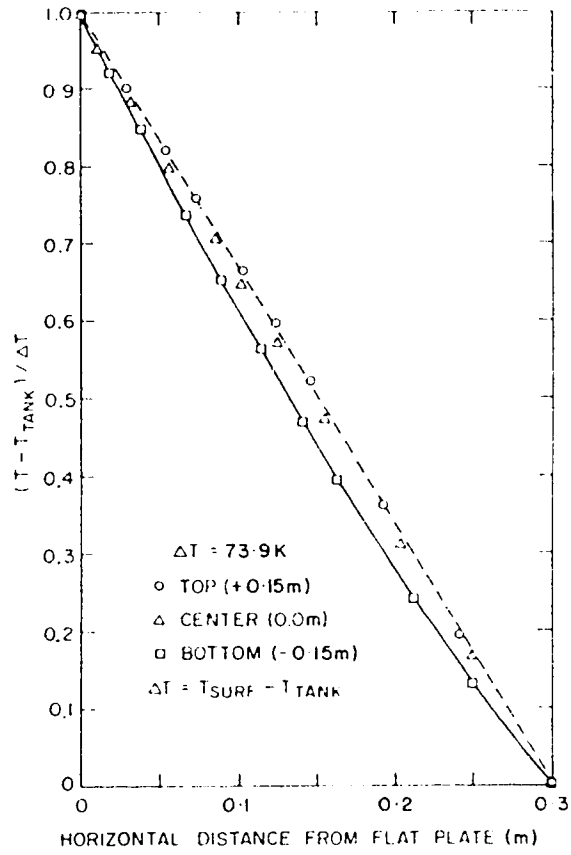
Figure 1.6 *Horizontal temperature profiles in a vertically situated glass fibre batt ($\Delta T = 73.9°C$).*

8

air at its top surface were studied. For the apparatus and experiments of Fig.1.7 observed temperature profiles are shown for the case of no imposed flow, for the case of free steam of air at 1.3 m/s parallel to the open surface, and for the case of free stream flow of air at 3.0 m/s at 45 deg with the horizontal. The experimental results showed that natural convection in sealed permeable insulators could occur and that natural convection as well as air intrusion into partially sealed permeable insulators could degrade the effective R-value of a permeable insulator.

Dale and Ackerman (1991) conducted a study to determine the effect of ventilation air flow on the performance of glass fibre insulation in the corner region of an attic as shown in Fig.1.8. Temperature measurements were made on the interior surface of the drywall and within the insulation. Figure 1.8 shows the locations of the thermocouples fitted inside the insulation. Results showed that the effectiveness of the insulation in reducing heat transfer was reduced substantially by air being forced through the insulation in the corner region. The effective R-value was reduced by a factor of 2 for the given conditions.

1.1   Scope of the Thesis

This study was initiated to investigate systematically the effect of air flow on heat transfer through porous insulation. The main emphasis, here, was to conduct controlled experiments in a small wind tunnel, and measure any change in heat flux through the insulation. A small sample of the insulation was mounted flush with the floor of a wind tunnel and the air velocity was varied up to 9 m/s. Both heat flux and temperature distributions were measured at several locations within the sample. From these measurements, an effective thermal resistance was calculated. Several different samples of insulation were tested with varying permeability which is related to the density of the insulation.

The material presented in this thesis is divided into five chapters. Chapter 1 presented a brief review and set the scope of the thesis work. Chapter 2 reviews some basic theory used to develop the foundations and background for the experiment analysis.
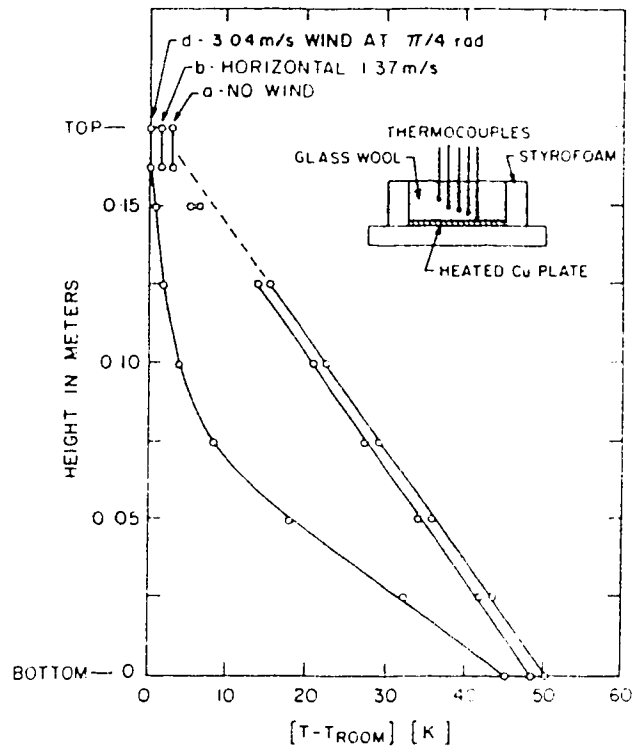
Figure 1.7 *Glass wool batt insulated and sealed on sides; heating at the bottom.*
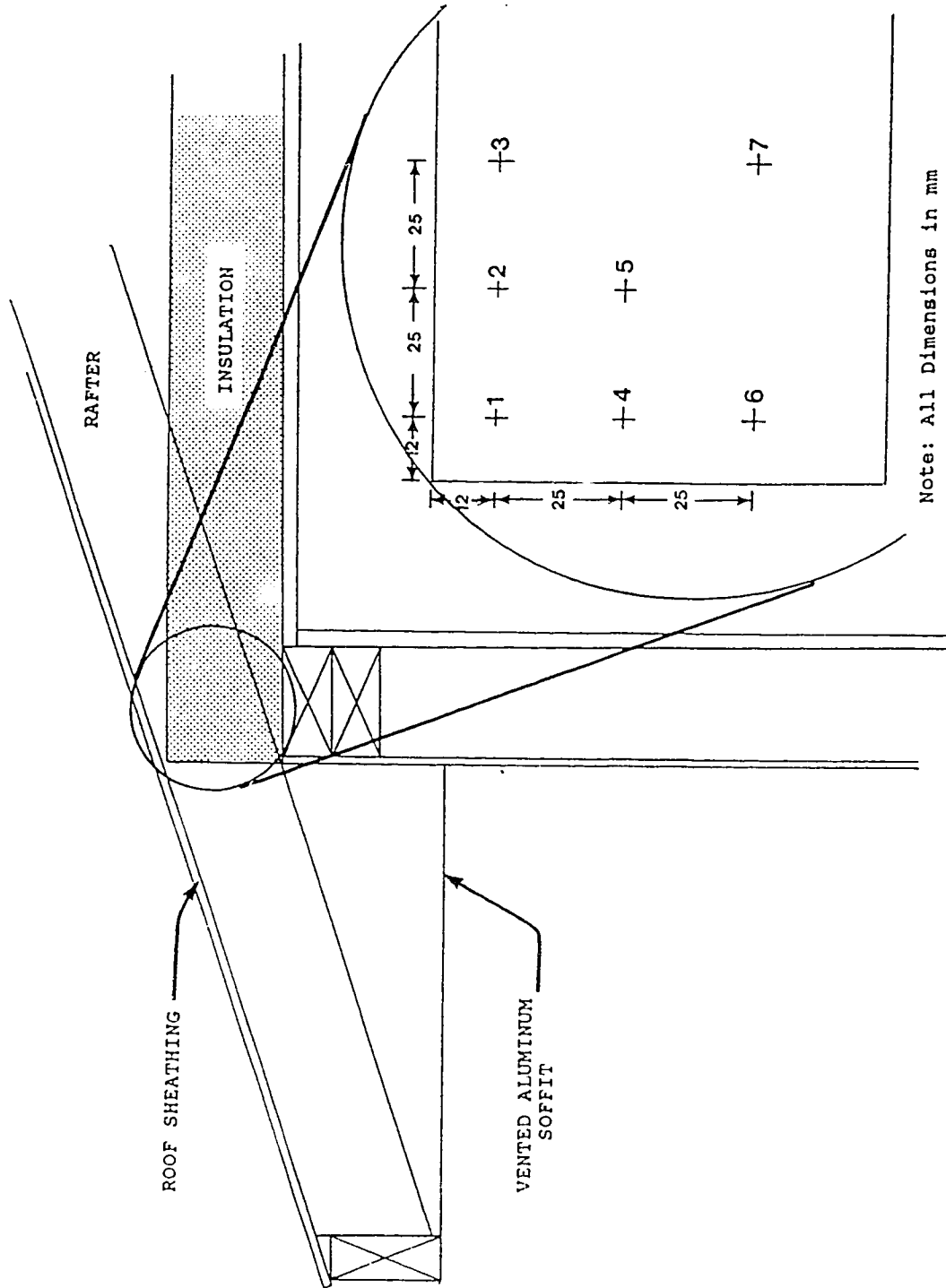
Figure 1.8 *Schematic showing the placement of thermocouples in corner region of attic insulation. (After Dale and Ackerman, 1991).*

This includes the flow of fluids through porous media and the effect of convective flow on temperature distribution in porous media. Chapter 3 combines a brief description of the design of the experimental apparatus, the measuring techniques, and the experimental procedures. A discussion of results of the tests including temperature distribution, and heat flux through the insulation are considered in Chapter 4. Finally, conclusions and recommendations for further study are presented in Chapter 5.

THEORY AND BACKGROUND

In this chapter, some of the fundamental aspects of flow and heat transfer in porous media applied to the scope of this thesis, are briefly discussed. The first deals with the flow through porous media as described by Darcy's law where the concept of per..neability is introduced. The second involves the flow of heat through porous media which is governed by the energy equation including conduction and convection. The effect of flow on temperature distributions within porous insulation is derived for two distinct flow situations: air flow parallel to heat flux and perpendicular to heat flux. These cases represent two extreme cases of air motion that are induced in porous medium due to air flow over the exposed surface of the insulation. This analysis will help to interpret qualitatively the temperature distributions that are presented in Chapter 4.

2.1 Darcy's Law for Flow Througin Porous Media

Darcy's law was developed to represent quantitatively the behaviour of fluids flowing through porous media. Based on experiments, Darcy, (Bejan, 1984), in 1856 concluded through experimental observations, the following relationship for flow through porous media:

$$u = -\frac{K}{\mu}\frac{dp}{dx} \qquad \qquad 2.1$$

where u is the velocity in the x-direction, dp/dx is the pressure gradient, K is a constant characteristic of the medium defined as permeability, and μ is the dynamic viscosity of the fluid flowing through the porous medium.

This law states that *macroscopically*[1], the velocity of a fluid flowing through a porous medium is directly proportional to the pressure gradient acting on the fluid. Darcy's law is valid when the volume-averaged velocity is small. This criterion is usually expressed in the form of a Reynolds number which is based on the length scale, $K^{1/2}$. For Darcy's law to be valid

$$Re = \frac{u_m \, K^{1/2}}{\nu} < 1;$$

where ν is the kinematic viscosity. For typical situations encountered in leakage air flow through insulation in houses, Nikel (1993) found u_m to be on the order of 0.01 m/s. Based on this velocity and K which is typically on the order of 10^{-9} m^2 for glass fibre insulation, the Reynolds number is 0.03. This shows that the Darcy's law is valid for the case presented in this thesis.

As pointed out by Muskat (1937), the direct experiment relating to Darcy's law was restricted to a column or beds of porous material in which the macroscopic flow is necessarily of a one-dimensional character. It is, however, necessary to generalize this empirical result to two-dimensional flow. The resultant velocity at any point is directly proportional to the resultant pressure gradient at that point. In the absence of body forces, Darcy's law in two dimensions is

$$u = -\frac{K}{\mu}\frac{\partial p}{\partial x}$$

$$w = -\frac{K}{\mu}\frac{\partial p}{\partial z}$$

2.2

where u and w are the velocities in the x direction and z direction respectively.

---

[1] The qualification *"macroscopically"* means that the volume element to which the velocity and pressure refer are suppose to contain a large number of pores and the dynamical variables are averaged over a large number of pores.

The permeability K may vary from point to point and may be different for the two components of the velocity. However, it will generally suffice to consider the medium to be isotropic (the case of this thesis), and K shall hereafter be taken as independent of direction.

For the case of one-dimensional flow through a porous medium under the action of uniform pressure gradient, Darcy's law reduces to

$$u = \frac{K}{\mu} \frac{\Delta P}{d}$$

2.3

where d is the thickness of the porous layer and ΔP is the pressure difference imposed across the porous layer. This equation will be used in Chapter 3 to measure the permeability, K.

2.2 Energy Equation

In order to calculate steady-state temperature distributions within a porous medium (or any medium), the energy balance including convection and conduction yields (Bejan, 1984)

$$u \frac{\partial T}{\partial x} + w \frac{\partial T}{\partial z} = \alpha \left(\frac{\partial^2 T}{\partial x^2} + \frac{\partial^2 T}{\partial z^2} \right)$$

2.4

where α is the thermal diffusivity defined as

$$\alpha = \frac{k}{\rho c_p} .$$

To help interpret the measured temperature profiles that will be presented in Chapter 4, two extreme cases are presented together with analytical solutions for the temperature

profiles. For both cases a horizontal porous layer of thickness d has a temperature gradient imposed on it by maintaining the bottom surface of the layer at T_w and the top at T_c; in both cases, T_w is greater than T_c. Case (a) has uniform air flow *parallel* to the direction of heat flow, while case (b) consider uniform air flow *perpendicular* to the heat flow. These are the two extreme cases considered.

2.2.(a) Air flow parallel to heat flux

The case is shown in Fig.2.1 where a porous layer has two horizontal surfaces kept at different temperatures. Heat transfer is in the vertical upward direction and air flows vertically downward through the upper surface. For the one-dimensional steady state Eqn.2.4 reduces to

$$w\frac{dT}{dz} = \alpha \cdot \frac{d^2T}{dz^2} \qquad 2.5$$

Equation 2.5 for temperature was solved analytically for the case where the boundary conditions are:

$$T\ (z=0) = T_w$$
$$T\ (z=d) = T_c \qquad 2.6$$

The analytical solution to Eqn.2.5 satisfying the boundary conditions yields the temperature distribution

$$T(z) = T_w + \left\{ \frac{T_w - T_c}{1 - \exp(\frac{w}{\alpha}d)} \right\} \left[\exp(\frac{w}{\alpha}z) - 1 \right] \qquad 2.7$$
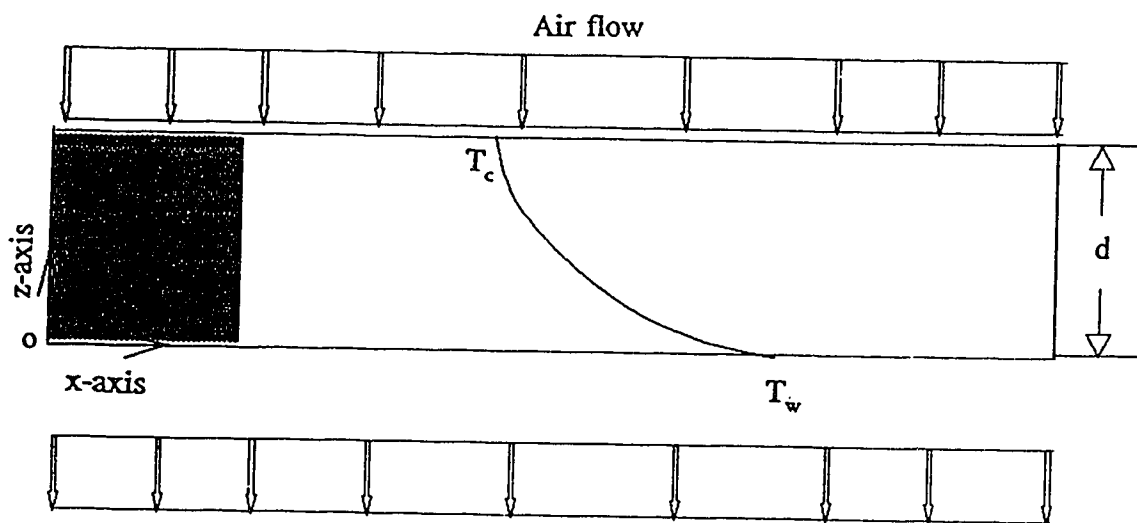
Air flow

Figure 2.1 *Porous medium with vertical air flow.*

The effect of various flow velocities was calculated for the typical case where

c_p = 1.0057 kJ /kg.°C,

k = 0.042 W/m.°C,

ϱ = 1.17 kg /m³ air at 1.01 atmospheric pressure and a temperature of 23°C,

T_c = 23 °C,

T_w = 47 °C,

w = 0.001 m/s, 0.0005 m/s, and -0.001 m/s.

d = 89 mm.

Figure 2.2 shows the temperature profiles for the typical conditions listed above for two velocities in the direction of the imposed temperature gradient, and one velocity opposite to the temperature gradient. For an imposed temperature across the medium, an increase in the flow velocity results in a deviation of the temperature profile from the linear profile. For the case where the imposed velocity is in the same direction as the heat flux, the temperature profiles deviate to the left side indicating an increase in temperature within the medium. However when the velocity direction is in the opposite direction of heat flux, the temperature profile deviates to the other side of the linear profile indicating a decrease in temperature within the medium. In both cases an imposed velocity affects the temperature within the medium and, therefore, on the heat flux for an imposed temperature across the porous layer.

2.2.(b) Air flow perpendicular to heat flux

In this case, a horizontal porous layer is bounded by two isothermal planes maintaining a vertical temperature gradient. Uniform air flow is imposed in a horizontal direction as shown in Fig.2.3. The governing equation for temperature was solved analytically for the case where the boundary conditions on the warm side was T_w, while on the cold side the temperature was T_c. The steady state energy equation reduces to
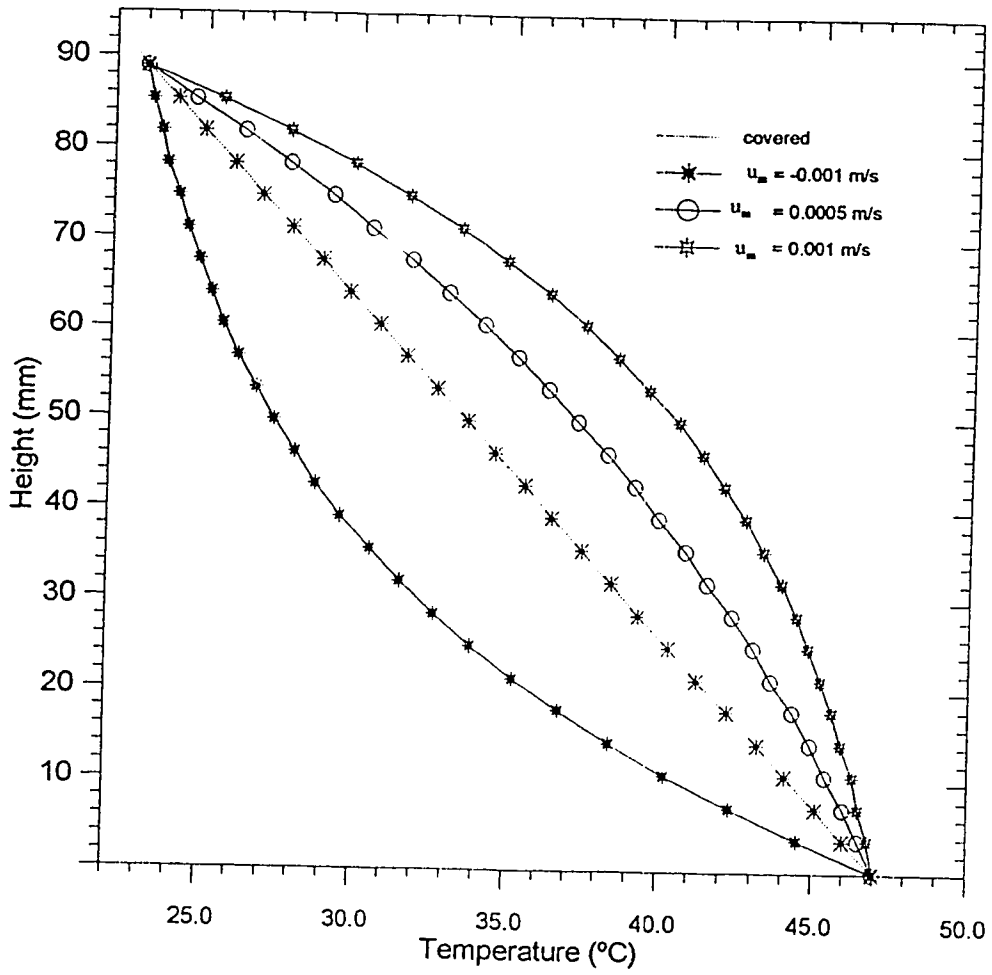
Figure 2.2 *Temperature profiles for the typical conditions of case 2.2(a).V*
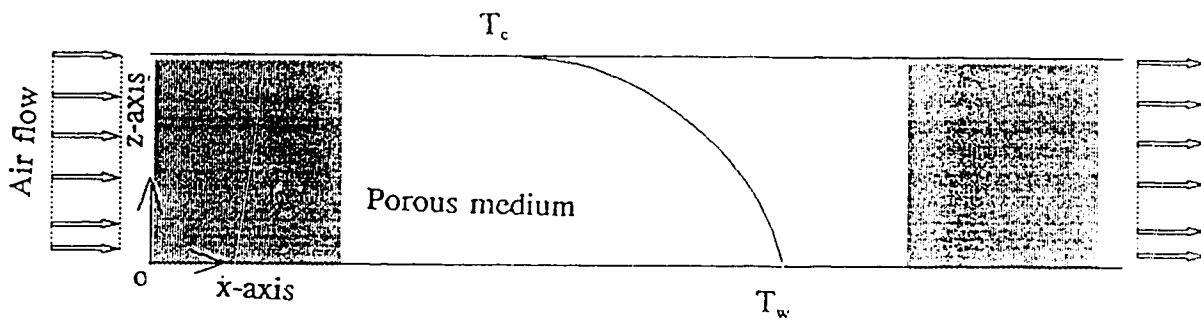
Figure 2.3 *Porous medium with horizontal air flow.*

$$u\frac{\partial T}{\partial x} = \alpha\frac{\partial^2 T}{\partial z^2} \qquad\qquad 2.8$$

subject to the boundary conditions defined by

$$T(x,0) = T_w$$

$$T(x,d) = T_c \qquad\qquad 2.9$$

$$T(0,z) = T_e$$

The last condition allows the air to enter the horizontal layer at temperature T_e different from T_w or T_c. Heat transfer between infinite walls with flow was discussed by McCuen (1962), Reynolds *et al.* (1963), and Lundberg (1963). Forest *et al.* (1993) used the solution method presented by McCuen (1962) to solve for the temperature distribution for the case under consideration. The analytical solution is

$$T(x,z) = (T_w - T_c)\left\{1 - \frac{z}{d} + \sum_{n=1}^{\infty} 2\left[\frac{T_c - T_e}{T_w - T_c}\frac{\cos(n\pi)}{n\pi} + \frac{T_e - T_w}{T_w - T_c}\frac{1}{n\pi}\right]\sin\left(\frac{n\pi}{d}z\right)\exp\left[\frac{-\alpha(n\pi)^2}{ud^2}x\right]\right\} + T_c \qquad 2.10$$

The effect of various flow velocities was calculated for the typical case where

$c_p = 1.0057$ kJ /kg.°C,

$k = 0.042$ W /m.°C,

$\varrho = 1.17$ kg /m³ at 1.01 atmospheric pressure and temperature of 23°C,

$T_e = 23$ °C,

$T_c = 24$ °C,

$T_w = 47$ °C,

$u = 0.001$ m/s and 0.005 m/s.

$d = 89$ mm.

Figure 2.4 shows the temperature profile for the typical conditions listed above for two velocities in the direction of the imposed temperature gradient. For an imposed
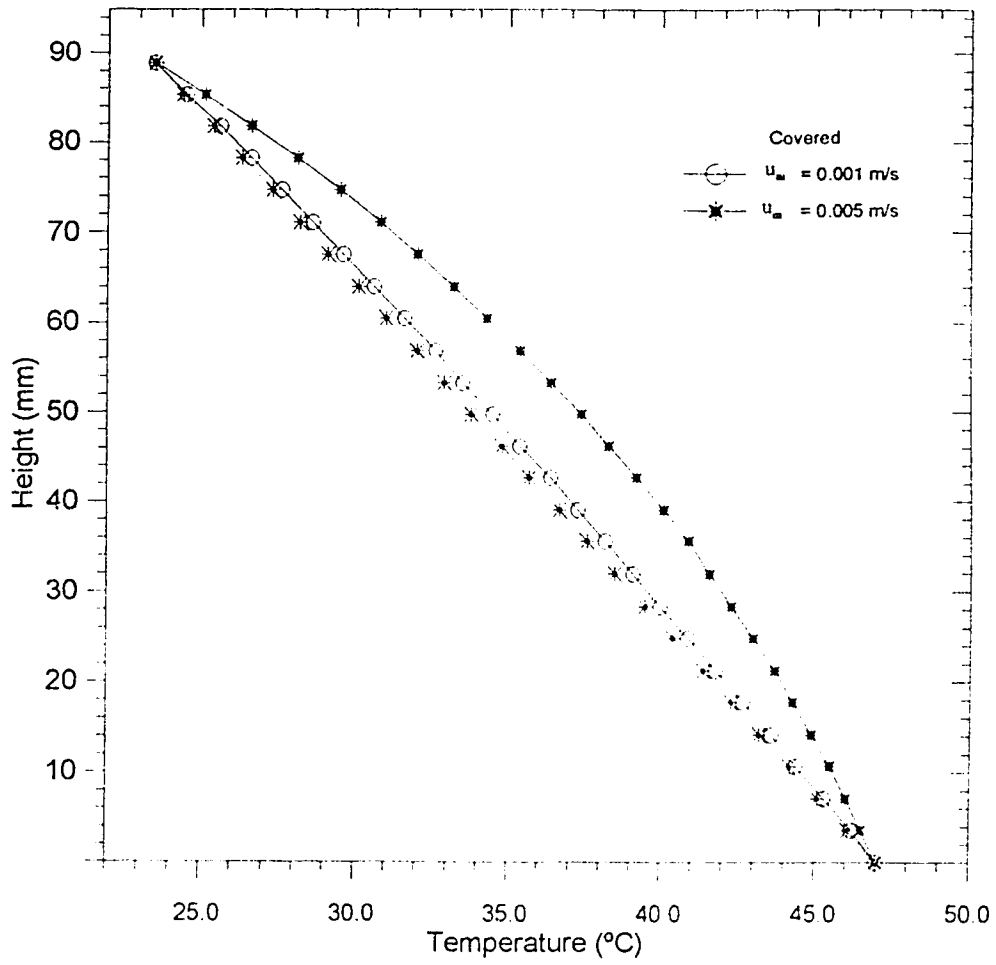
Figure 2.4 *Temperature profiles at location, x, equals 25 mm for the typical conditions of case 2.2(b).*

temperature difference across the medium an increase in the flow velocity results in a deviation of the temperature profile from the linear profile. Air flow affects the temperature profile within the medium and thus, alters the heat flux across the porous layer for an imposed temperature difference. This shows the manner in which heat loss rates through partially sealed permeable insulators can increase as the velocity increases. This result will be used in Chapter 4 to help interpret the experimental results.

2.3   Stability

In the preceding analysis, the horizontal porous layer was heated from below. It is well know that the existence of a temperature gradient parallel to the gravity vector may give rise to fluid movement. This fluid movement (natural convection) leads to flow instability characterized by Benard convection (natural convection) if the imposed temperature difference exceeds a critical value. A stability analysis for this situation was given by Horton and Rogers (1945), Lapwood (1948), and Bejan (1986) for a porous media. The critical condition for the onset of natural convection is expressed in terms of a Darcy-modified Rayleigh number defined as

$$Ra = \frac{g\beta K(T_w - T_c)d}{\alpha \nu} \qquad 2.11$$

where g is the gravitational acceleration, $\beta = 1/T$ is the coefficient of thermal expansion of air, d the porous medium thickness, T_w and T_c are the temperatures of the bottom and upper surface of the sample respectively, and α is the thermal diffusivity of the fluid saturated medium. Stability analysis shows that the onset of natural convection motion corresponds to a critical Rayleigh number, Ra_{cr} of $4\pi^2$. From an enginering heat transfer standpoint, for a Rayleigh number less than approximately 40, the heat transfer rate is accurately predicted by pure conduction. For Rayleigh numbers much larger than 40, natural convection has to be taken into consideration.

For the range of permeability, K, used in this study ($K = 2.4 \times 10^{-8}$ m^2 to 5.4×10^{-9} m^2), the critical temperature difference for a porous layer of thickness $d = 89$ mm between two horizontal rigid boundaries varies from 76°C to 340 °C. This critical temperature difference is much larger than the temperature difference range used in this study. This calculation shows that a large ΔT is required to induce natural convection within the porous layer, and that the effects of natural convection can be neglected in this study.

EXPERIMENTAL APPARATUS AND TEST PROCEDURE

In this chapter, the experimental apparatus and procedures for determining the effect on heat transfer of air flow over the exposed surface of porous insulation are described. Tests were conducted in a small, open (non-recirculating) low speed wind tunnel. The exposed surface of the insulation was mounted flush with the floor of the tunnel. The bottom of the insulation was heated electrically by maintaining a constant temperature above the ambient temperature. Temperature profiles and heat fluxes were simultaneously measured for a number of mean tunnel velocities. These tests were repeated for insulation with varying permeabilities. The experimental apparatus and test procedure are described in this chapter.

3.1   Wind Tunnel

The wind tunnel used in the experiments was a small non-recirculating tunnel with a working cross section 305 mm by 305 mm; the lenght of the test section is 920 mm. Air from the room was drawn in by a fan mounted at the end of the tunnel; at the inlet, a bell-mouth and flow straighteners (a honeycomb and screens) ensured a uniform velocity profile. The air, then, entered a nozzle where its velocity was increased. To provide a gradual transition from the nozzle to the test section, the air came in through a straight square section (305 mm x 305 mm). The air was continuously exhausted to the room by means of an axial flow fan (AEROVENT, Type CDE 1 31643) connected to a 10 horse-power electric motor. The velocity in the tunnel was varied by opening or closing a gap between the end of the tunnel (diffuser) and the fan assembly. The flow velocities in the test section varied from approximately 0.8 m/s to 12 m/s. Lower velocities than 0.8

m/s were achieved by adding more resistance to the inlet using a large mat of filter fibre. This allowed velocities down to 0.4 m/s. A schematic of the model is given in Fig. 3.1. The flow-velocity was measured with a pitot-static tube attached to a differential pressure transducer (Validyne Model DP 45-16). In order to average the pressure fluctuations, the output of the transducer was measured with an averaging voltmeter. An averaging time of 100 sec was used for all velocity measurements. The pitot tube was mounted on a positioning device that allowed the pitot tube to be positioned at a desired height above the insulation sample. A set of a typical velocity profiles in the tunnel are shown in Fig.3.2. As can be seen from Fig.3.2, over a large part of the cross section the velocity is approximately uniform, forming a large "core" below which the tested body was placed. Outside this core the velocity decreases to zero at the walls. Mean velocities were measured at a height of 153 mm above the exposed surface of the insulation.

3.2   Insulation Sample Holder

The insulation sample was mounted in a metal box so that the upper surface of the insulation was flush with the floor of the tunnel in the test section. It consisted of a large rectangular 711 mm long x 406 mm wide x 153 mm deep metal box to hold the body of the sample. A schematic diagram is given in Fig.3.3. The vertical sides of the box were insulated with 51 mm thick (RSI = 1.76) rigid foam insulation to reduce the lateral heat loss. Two 25 mm thick plexiglass plates were bounded to the longitudinal sides of the box where the thermocouple arrays were held in place. The sample holder was attached and sealed to the bottom of the tunnel so that no air leakage occurred. The san.ple spanned the full width of the tunnel; the sample thickness was set to 89 mm which is approximately a standard thickness for glass fibre insulation. The sample was located approximately 2.5 m from the inlet of the tunnel.

3.3   Heaters and Control System:

The insulation sample (Fig.3.4) was heated from below using an electrical sheet
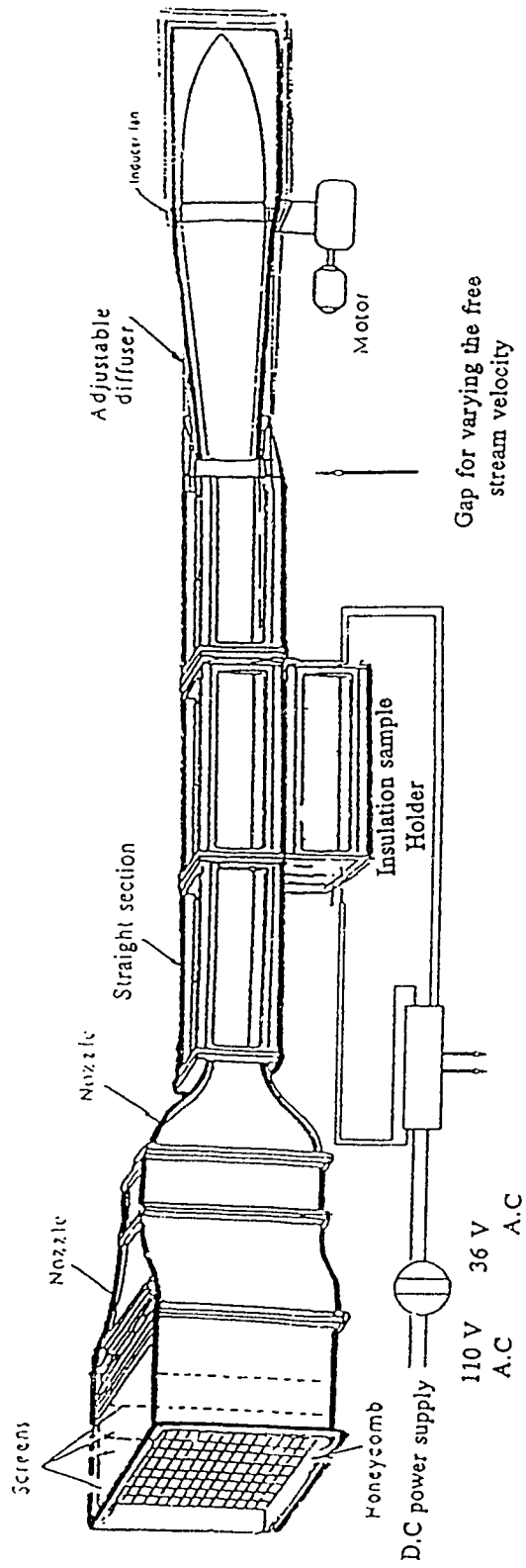
Figure 3.1 *Low speed wind tunnel with the insulation sample.*

27
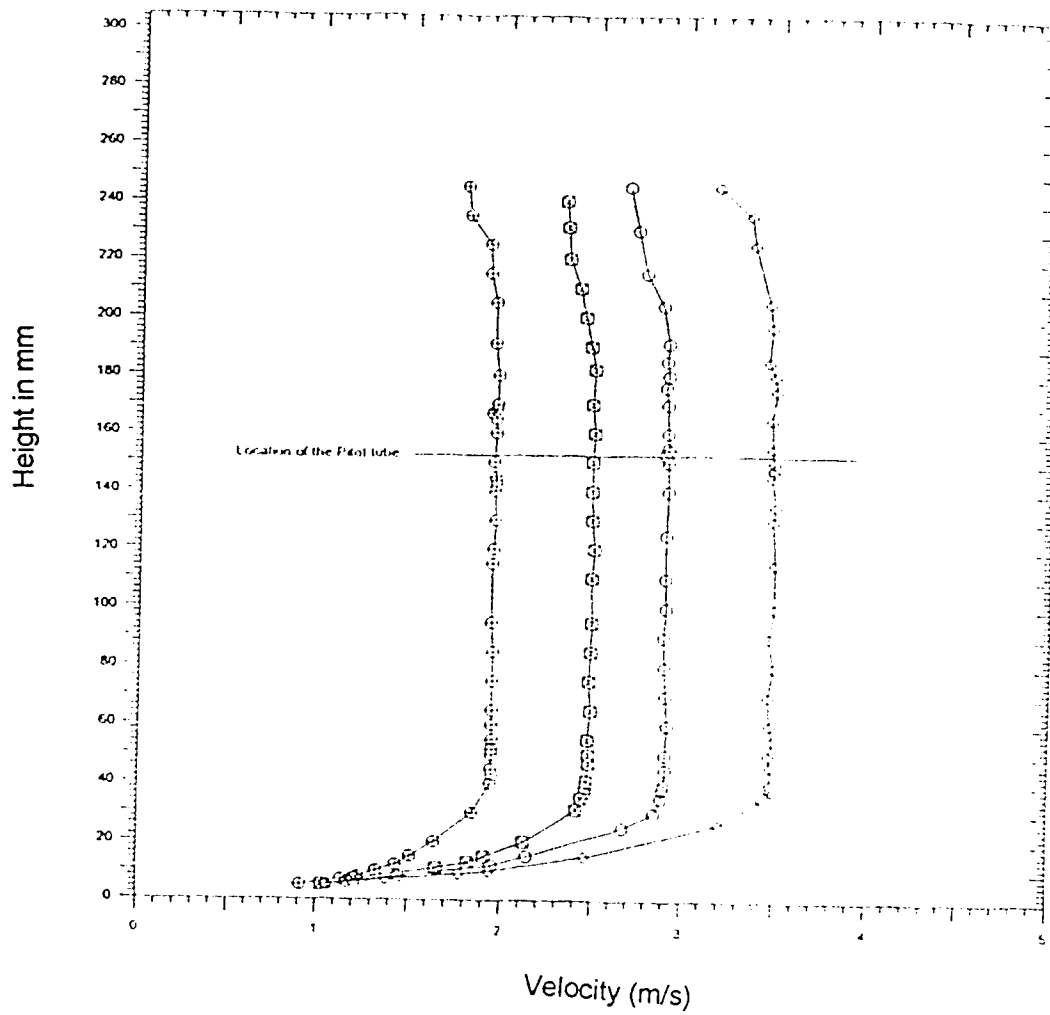
Figure 3.2 *Vertical profiles of free stream velocity in the test section of the wind tunnel. Measurements taken at distance of 305 mm from the leading edge, 153 mm from the floor of the tunnel, and 153 mm form the lateral sides of test section.*

POROUS MEDIUM

305

51

711

610

95

153

406

25

HOLES FOR GUIDING
THERMOCOUPLES
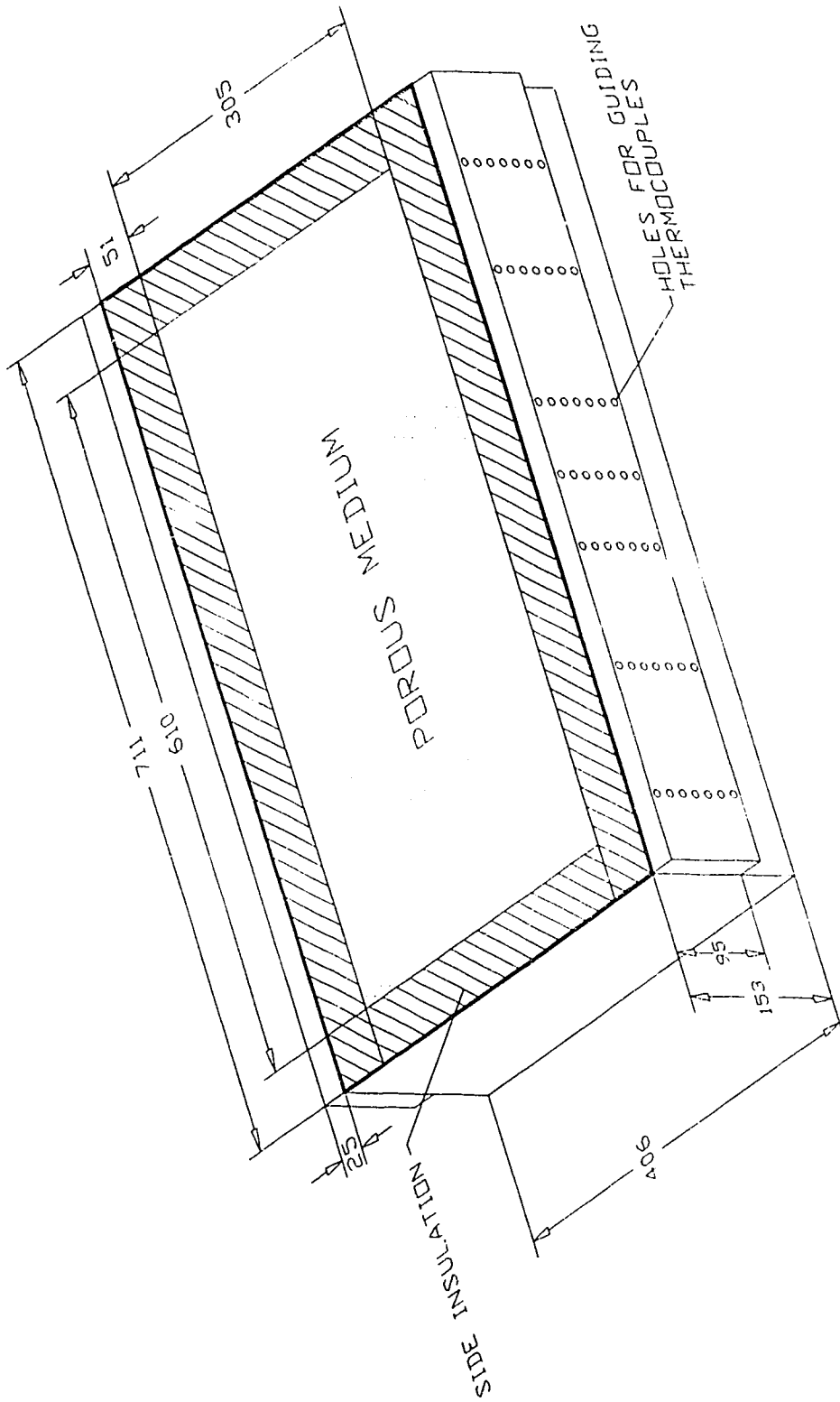
SIDE INSULATION

Figure 3.3 *Insulation sample holder. All dimensions are in mm.*

29

heating element. The heating element (OMEGALUX model SRFG-1224) was 610 mm x 305 mm and could generate a maximum heat flux of 720 W. It was connected to a metered power supply (KROHN-HITE Model UHR-T361OR, D.C 0-36 volts, 0-10 amps). The power input to the heating element was controlled by a variable transformer in order to maintain a constant plate temperature. The temperature of the plate could be controlled to within ± 1.5°C of the desired temperature. The bottom side of the heater was bounded by a layer of plexiglass 13 mm thick. In order to minimize the heat loss to the bottom of the holder, a similar heater was placed on the bottom of the plexiglass layer. The two heaters were connected to a temperature difference controller and maintained at a fixed ΔT of 7°C. Plate temperature sensors (AD 594 transistor sensors) were placed in the middle of the plate. In order to ensure that the heaters were at uniform temperature, the heaters were bounded to thin (1 mm thick) copper plates. The main heater was separated from the bottom of the insulation by a 4.4 mm air gap. The air gap was used for measuring heat flux as detailed in Sec. 3.5.

3.4   Temperature Measurements

In order to determine the effect of air intrusion on heat transfer through the insulation, temperature profiles were measured at seven locations along the sample as shown in Fig.3.5. At each location the temperature profile was measured with an array of 8 copper-constantan thermocouples (28 gauge). Thermocouples were installed in thin metal guide tubes which allowed the thermocouples to be accurately located in the insulation. In addition by pushing in the metal tubes, the temperature profiles at any location across the width of the tunnel were obtained. Seven thermocouples were taped on the heated plate to provide its temperature distribution. In all tests, the maximum difference between the seven readings was less than 2°C, therefore, the average of the seven reading was taken as the plate temperature. For each experiment, with a measured heat input to the heating element, the output of the thermocouples was monitored using a computer-data acquisition system. The temperatures were recorded with an analog digital convertor (Sciemetric board, Model 641 D.C.) where temperature could be resolved
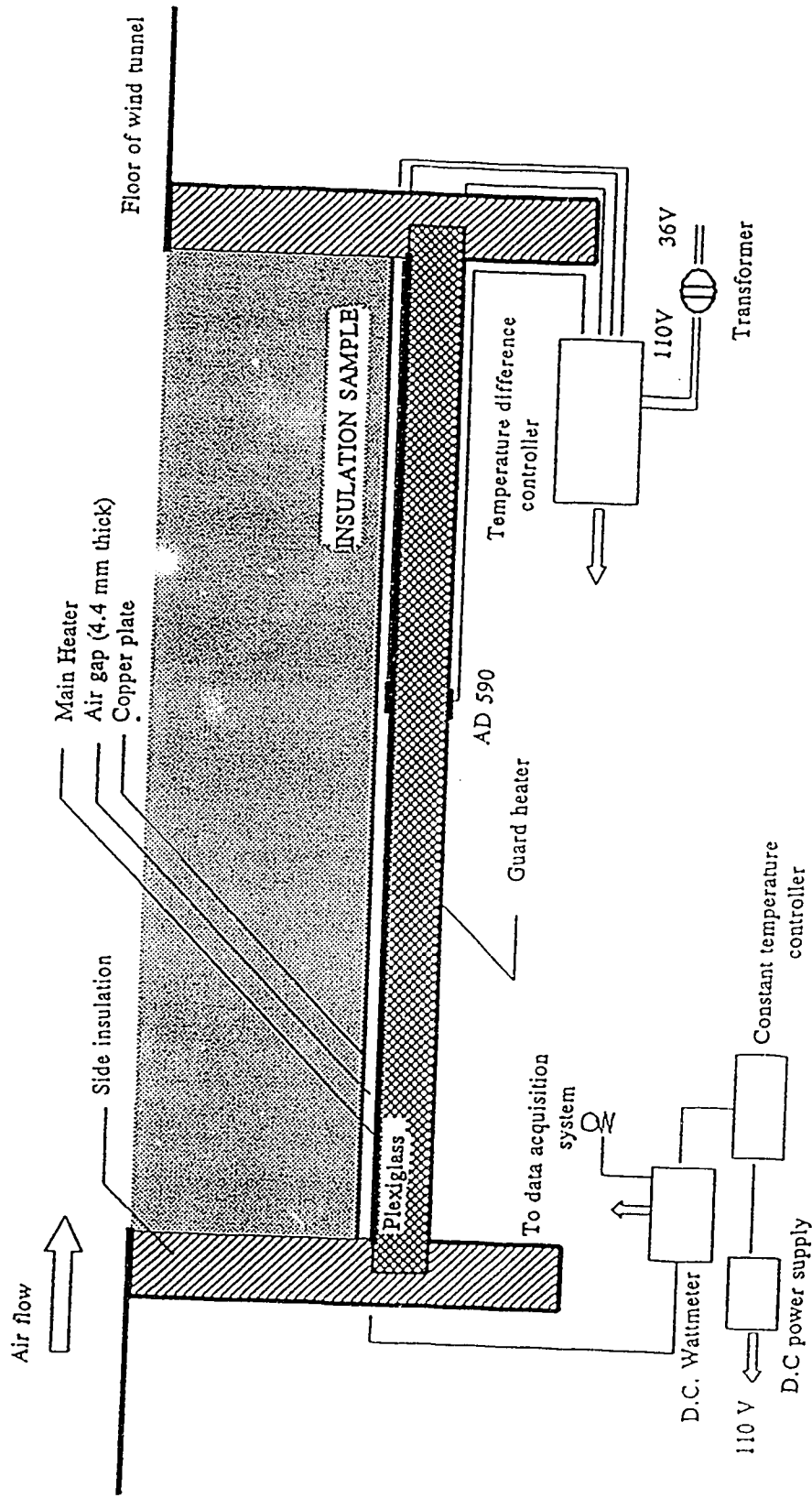
Figure 3.4 *Heaters, air gap, constant plate temperature controller, and temperature difference controller.*

31
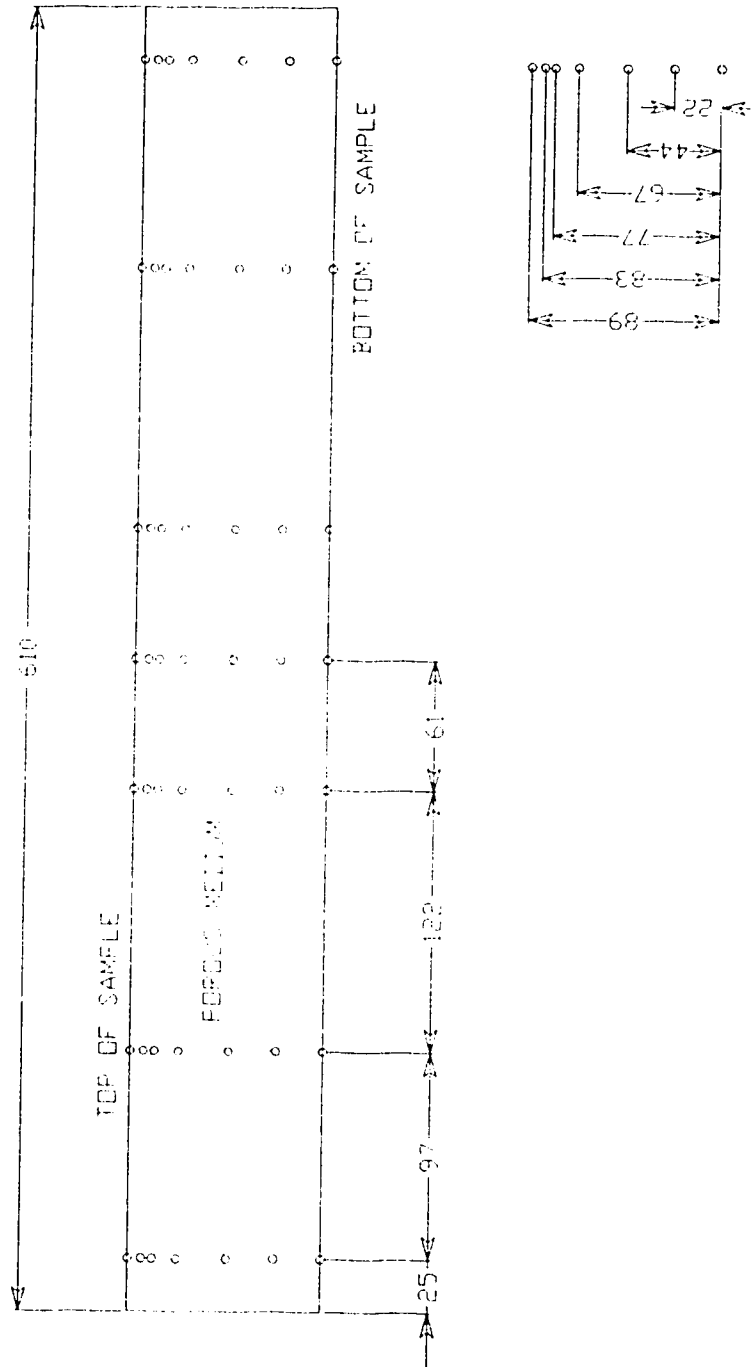
Figure 3.5 *Location of thermocouples in the insulation sample.*

32

to 0.03°C (0.05°F), and the measuring accuracy (including gain, A/D conversion , and reference temperature errors) was ± 0.5 °C (± 0.9°F). The thermocouples and data acquisition system were calibrated by placing the active junction in a temperature controlled calibration bath. Taking readings over a range 0 °C to 85 °C, the recorded temperatures were then compared with a digital thermometer (Fluke, model 2180 A RTD) also emersed in the bath. The combined data acquisition and measurement error was within ∓1.1 °C of digital thermometer reading.

3.5   Heat Flux Measurements

In order to evaluate the effective resistance of the insulation, heat flux through the insulation must be measured. As shown in Fig.3.4 the sample holder was equipped with a small air gap. The air gap of 4.4 mm thick was located between the main heater and the copper plate supporting the porous medium. This air gap was maintained in all sides with wooden strips (4.4 x 4.4 mm² cross section) sealed to the copper plates. The temperature difference across the air gap was measured at 4 locations. The heat flux across the air gap will be the sum of the heat transfer by conduction, convection and radiation. For the onset of natural convection in the air gap, the critical Rayleigh number defined as, (Bejan, 1984)

$$Ra = \frac{g\beta \; \Delta T \; d^3}{\alpha.\nu} \qquad\qquad 3.1$$

must exceed the value of 1108. For the given gap size,d equal to 4.4 mm, and air as the intervening medium, natural convection will set in when ΔT exceeds 140 °C. For all experiments, the maximum measured ΔT was less than 10 °C; thus, natural convection is not present. The last heat transfer mechanism is radiation. Modelling the air gap as two parallel infinite planes and assuming that the air is a transparent medium, the calculated radiation heat flux for a measured ΔT of 10°C was on the order of 0.042 W/m². This is

two orders of magnitude smaller than the conduction heat flux. Thus, the air is motionless and the heat flux can be calculated using pure conduction across the gap; that is

$$q = k_{air} \cdot \frac{\Delta T}{d}$$ 3.2

3.6   Testing Procedure

The insulation sample was properly installed and sealed in the test section of the wind tunnel, and the upper surface of the insulation was flush with the floor of the tunnel. Before starting any test, it was first established that the porous medium and the walls of the holder were all at ambient temperature. Then, a temperature difference across the insulation sample was established by increasing the power input to the main heater. After each new setting of the temperature difference the wall temperature and the heat flux were monitored in 3- to 5- minute intervals until equilibrium was reached, which was usually less than 30 min. The main heater temperature was set by adjusting the temperature controller. Three different plate temperatures of 47 °C, 60° C and 67°C were selected for the tests.

For each experimental condition, two tests were conducted. The first test involved covering the exposed surface of the insulation with a thin aluminium plate and measuring temperature profiles and heat fluxes after the system reached steady state. For this case, the temperature profiles in the insulation should be linear. In addition, the measurement procedure was corroborated by calculating the insulation thermal conductivity from the measured temperature gradient and heat flux. For the second test, the aluminum plate was removed exposing the insulation to the air stream; after steady state was reached, temperature profiles and heat fluxes were measured. Several tests were repeated to test the reproducibility and accuracy of the results.

Different insulation samples were tested with a range of permeabilities. The initial sample was a commercially available glass fibre insulation with a standard thickness of

89 mm. Subsequent tests were conducted with different samples consisting of glass fibre furnace filter material which has very high permeability. The filters are available in a standard 25 mm thickness. Thus several layers were placed in the holder to achieve a thickness of 89 mm. The permeability of these samples was varied by compressing more and more layers into the sample holder. Up to 20 layers of filter were placed in the sample holder. In Sec 3.7, the permeability of these different samples, was measured in a separate apparatus.

3.7   Permeability Measurements

The permeability, K, was calculated using the one-dimensional form of Darcy's law, Eqn.2.3. By measuring the pressure difference and flow rate of air through a sample with a given cross sectional area and length, K could be calculated.

The insulation sample was uniformly packed in a cylindrical tube. The holder was a cylinder 62 mm internal diameter and 178 mm long. Air was drawn through the sample holder and then through a positive displacement flow meter (DTM-115 SINGER) by means of a small air pump. A schematic of the flow apparatus is shown in Fig.3.6. The pump was adjusted to achieve a certain flowrate. For each sample the fowrate and pressure difference, ΔP, were set to several values in order to measure the dependence of flow on ΔP. The results, as shown in Fig.3.7, corroborate a linear dependance of flow on ΔP as Darcy's law requirs. The pressure across the sample was very small when taking the standard thickness, 89 mm; therfore, a thickness of 178 mm was chosen for all samples. Data for the commercial glass fibre insulation are shown in Fig. 3.7. From the slop of this figure, the measured permeabilty is 5.4 x 10^{-10} m^2. Th's measured value was compared with a correlation for K developed by Jackson and James (1986). The correlation was based on the mean filter diameter and volume fraction of solid material.
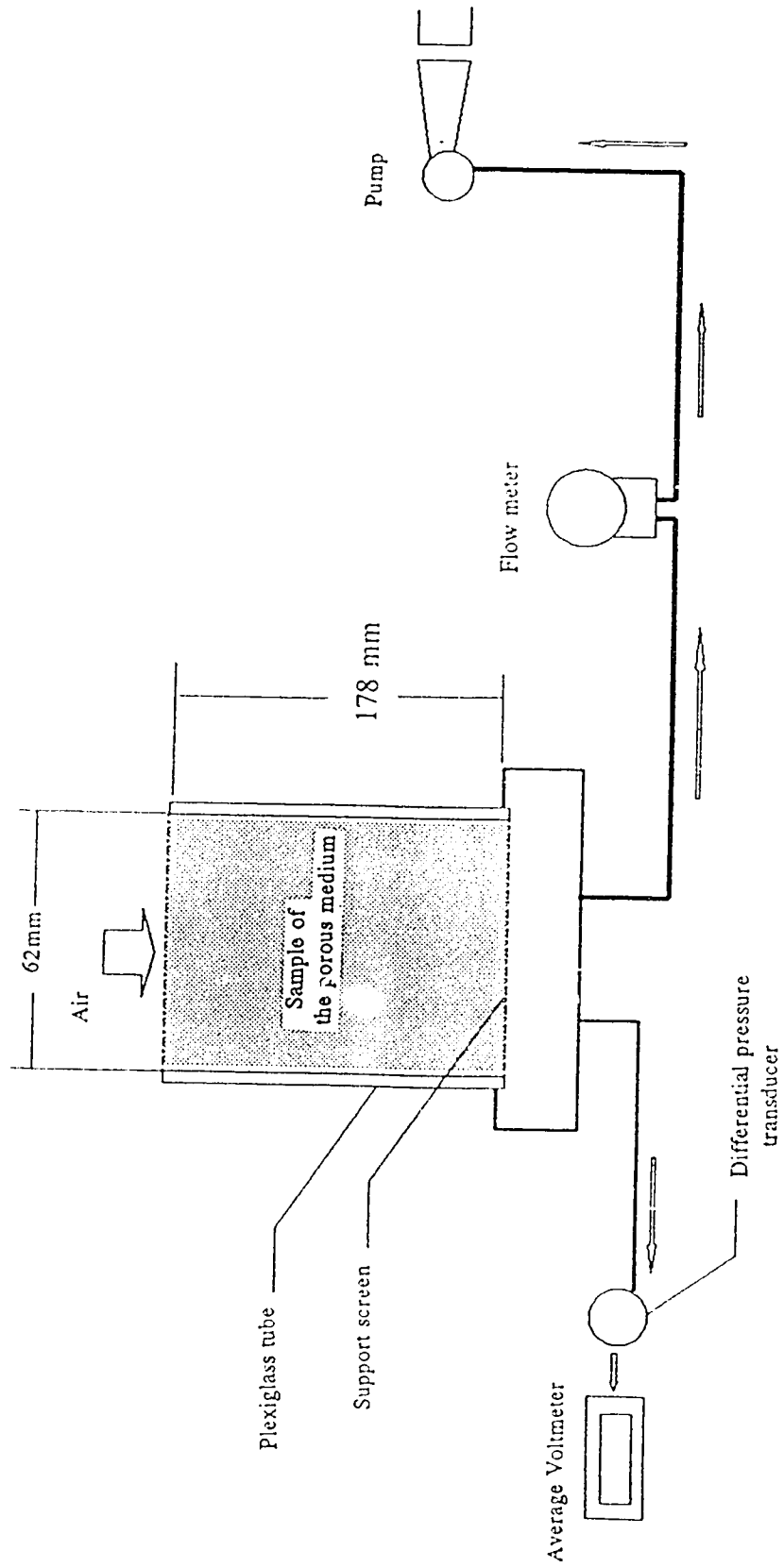
Figure 3.6 *Apparatus for permeability measurement.*
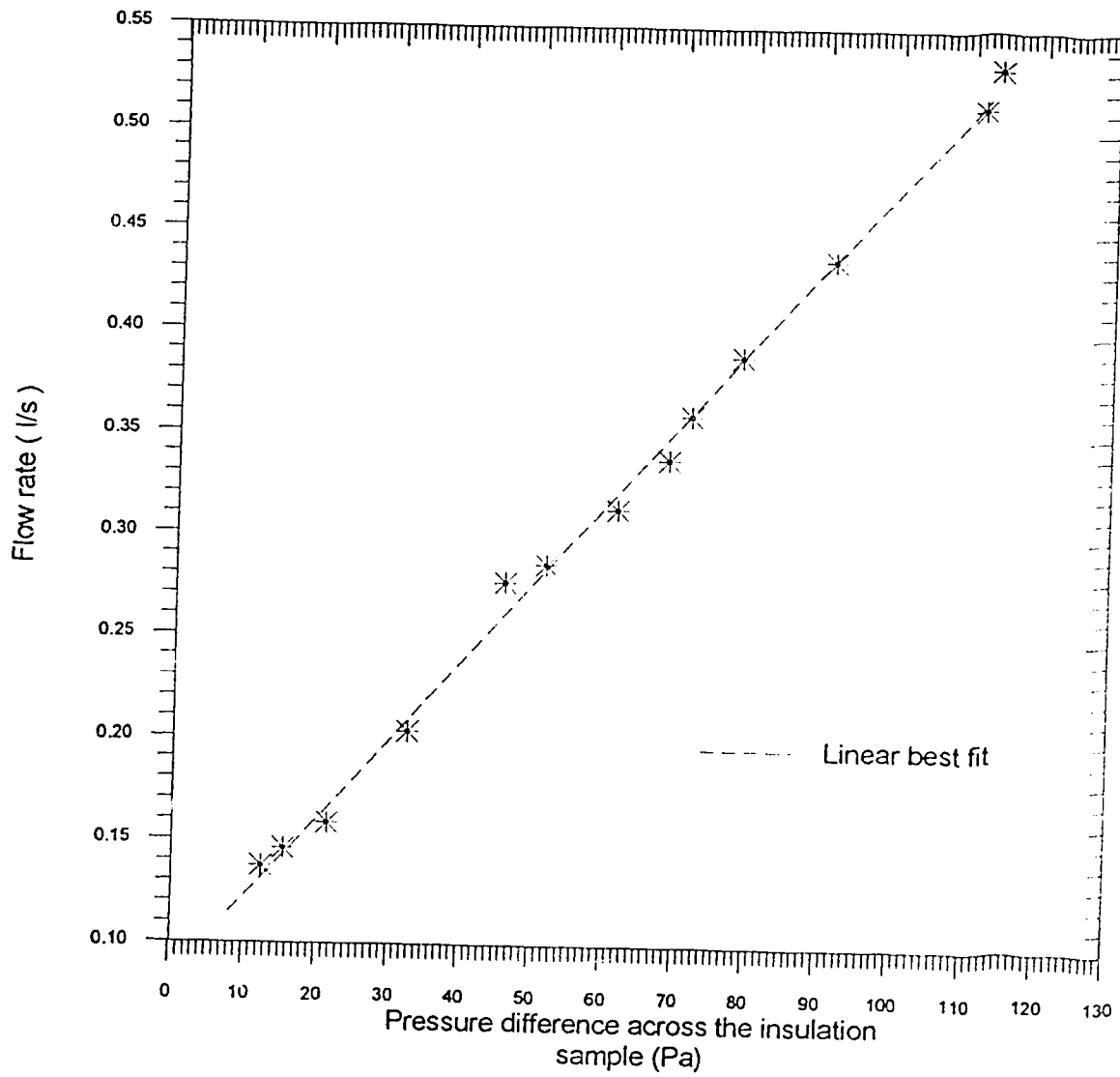
Figure 3.7 *Linear relation between flowrate and pressure across a sample of glass fibre..*

$$\frac{K}{a^2} = f(\phi) \qquad\qquad 3.3$$

where a is the mean filter diameter and ϕ is the volume fraction defined as

$$\phi = \frac{V_S}{V_T} \qquad\qquad 3.4$$

where V_S is the solid volume and V_T is the total volume of the porous medium. From the definition of ϕ the density of porous insulation can be related to the density of the solid matrix and density of air by

$$\rho = \rho_a(1 - \phi) + \rho_s\phi \qquad\qquad 3.5$$

where ρ_a, ρ_s are respectively the density of the air at room temperature and density of glass. For the commercial glass fibre insulation ρ_a is 1.17 kg/m^3 at room conditions and ρ_s is 2700 kg/m^3 (Holman, 1981). The mean fibre diameter, a, was measured by taking fibres from the insulation sample and measuring the diameter by using a microscope over a range of 30 fibres for both insulation samples. The value of diameter was found to be 17 x 10^{-3} mm for glass fibre and 31 x 10^{-3} mm for the glass fibre furnace filter material.

For the glass fibre insulation, the measured density was 11.2 kg/m^3, which yields a volume fraction ϕ of 0.0037. Using the Jackson and James correlation (Eqn.3.3), the estimated value of K for glass fibre insulation is 6.0 x 10^{-9} m^2. This value is very close to the measured value, 5.4 x 10^{-9} m^2. Similar measurements of density and permeabilities were carried out for glass fibre furnace filter material. These were tested at different densities. Results of the measurements and calculation of permeabilities are given in

38

Fig. 3.8. Figure 3.8 shows reasonably good agreement between the measurements and the Jackson and James correlation. The lower limit corresponds to a density of 0 kg/m^3 and permeability of infinity; the upper limit corresponds to a permeability of 0 m^2 which correspond to a solid medium.
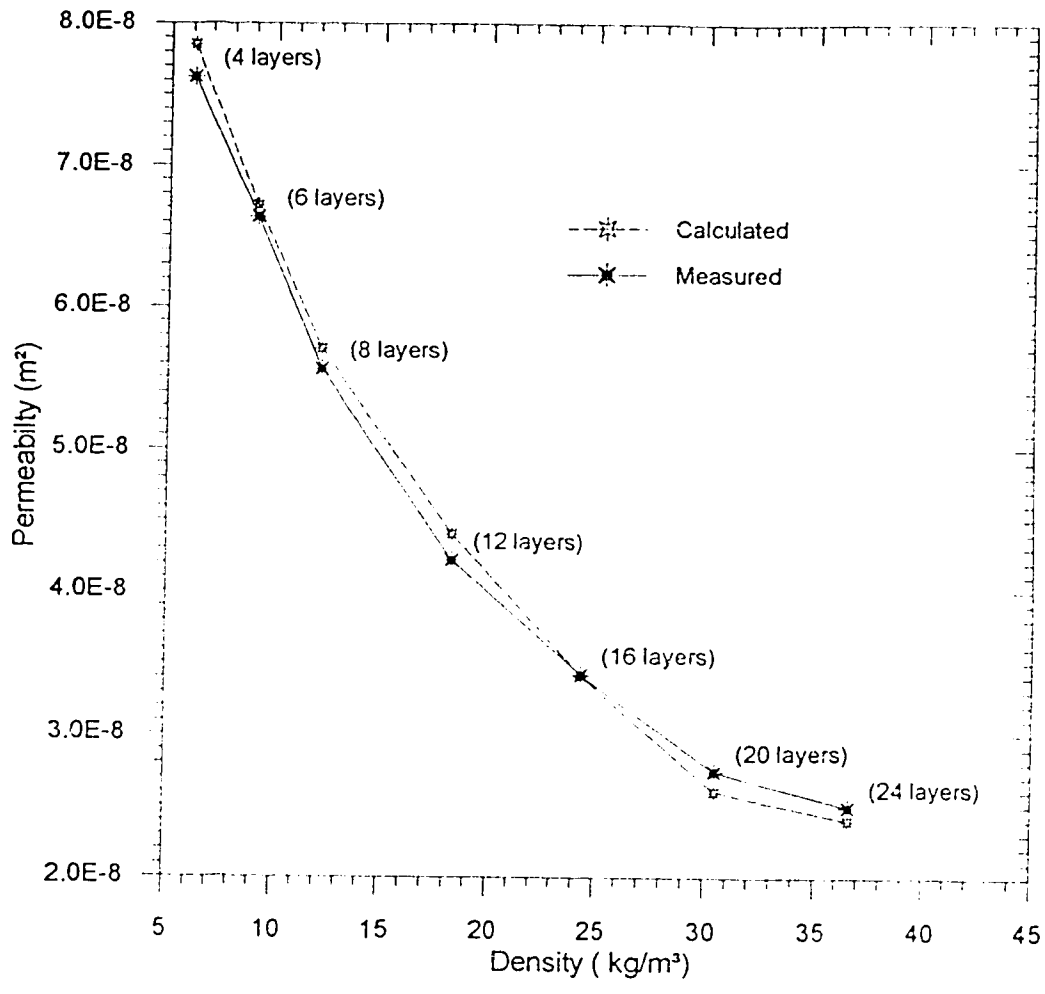
Figure 3.8 *Measured permeabilities for glass fibre furnace insulation. Measurements taken for a constant thickness of 178 mm.*

DISCUSSION OF RESULTS

The results of the experimental investigation concerning the effect of the air flow over porous media using a low speed wind tunnel are presented in this chapter. Measurements of temperature profiles and heat flux show that the effective R-value of the insulation decreased significantly with increasing free stream velocity. The non-linear temperature profiles within the insulation indicated that air flow was induced *within* the insulation as a result of the air flow over the exposed surface of the insulation.

4.1 Temperature Distribution Within the Insulation

In order to detect any changes in thermal performance of the insulation, temperature profiles were measured at different locations along three directions; x-direction (along the axial direction), y-direction (along the lateral length of sample), and z-direction (through the thickness of the sample). Figure 4.1 defines the axis-coordinates and origin. Two tests were conducted at each free stream velocity. The first test involved covering the exposed surface of the insulation with a thin aluminum plate and measuring temperature profiles and heat flux after the system reached steady state. For the second test, the aluminum plate was removed exposing the insulation to the air stream. After steady state was reached, temperature profiles and heat fluxes were measured. In each case, the temperature field in the porous medium was measured at various locations.

4.1.1 Lateral temperature variation (y-direction)

Figure 4.2 shows the measured lateral temperature profiles at four different locations, i.e. 25mm, 122mm, 244mm and 366 mm from the leading edge for the case

Air flow

Floor of the tunnel

z-axis

y-axis

Porous medium

O x-axis
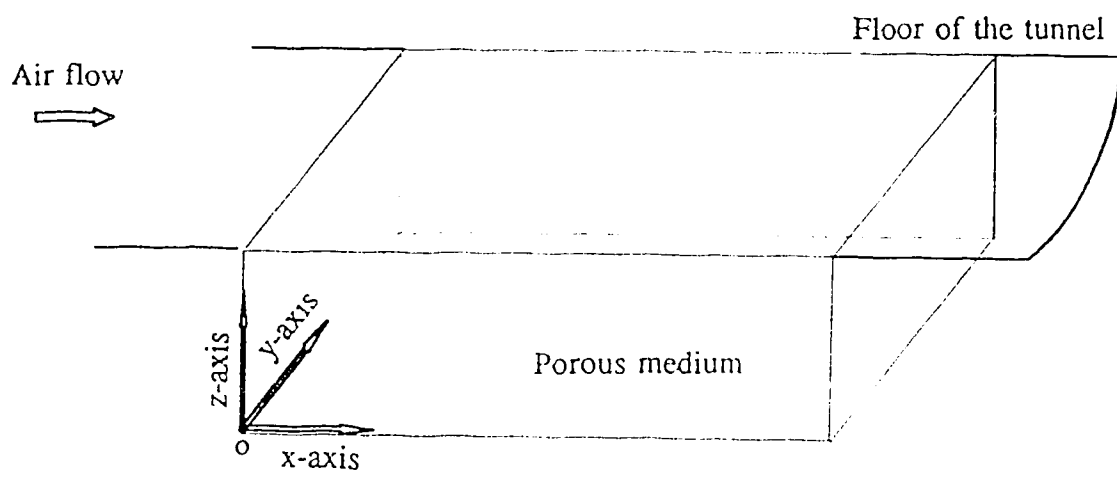
Figure 4.1 *Axis coordinates and origin used in this thesis.*
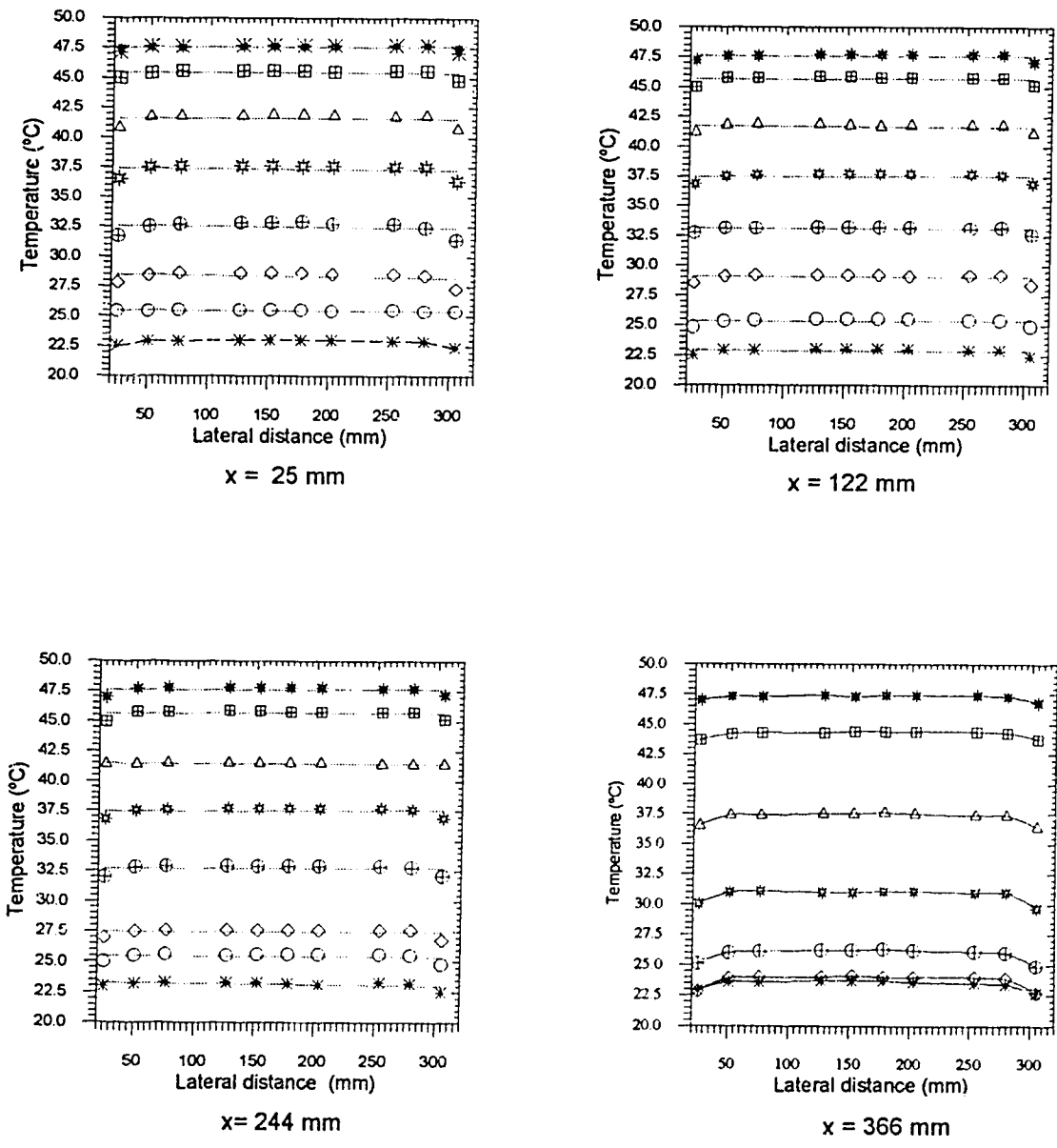
Figure 4.2 *Lateral temperature profiles for the glass fibre insulation sample covered with aluminum plate for different locations along the centre-line. The plate temperature is 47°C .*

43

where the glass fibre insulation sample was covered with the aluminum plate. This set of figures shows that except for a slight decrease in temperature at the edges of the sample there was no temperature variation in the lateral direction (y-direction). Essentially, the same results were obtained when the sample was uncovered.

Figure 4.3 shows the measured lateral temperature profiles at a location of 305 mm from the leading edge, for a range of velocities from 1.80 m/s to 5.09 m/s and a plate temperature of 47°C. For the exposed insulation, there is, again, very little change of temperature in the lateral direction except near the edge of the sample. A similar set of results showing little temperature variation in the lateral direction, was obtained at the plate temperatures of 60°C and 67°C. Based on these results, all subsequent temperature measurements were carried out only along the centre-line of the sample in order to minimize the amount of data collection.

4.1.2 Horizontal temperature variation (x-direction)

Figure 4.4 shows the measured horizontal temperature profiles along the centre line of glass fibre insulation for the case where the sample was covered and the plate temperature was 47°C. With the exception of the upstream and downstream edges, temperature profiles were constant in the axial direction. For the covered samples there was no indication of air motion within the sample. Thus, heat transfer should occur by conduction only. This is corroborated by the linear vertical temperature profiles presented in Sec 4.1.3. Figure 4.5 shows the axial variations (x-direction) in temperature when the glass fibre sample is exposed to air flow over the surface. This case is for a bottom plate temperature of 47 °C. In each of the six figures, the top profile corresponds to the temperature of the plate which can be seen to be at uniform temperature. In addition, the bottom profile corresponds to the temperature of the upper surface of the insulation sample. Again, the measurement shows that the upper surface temperature is more or less uniform. However, at intermediate locations within the sample, the temperature profiles are distinctly non-linear. Even at a low velocity of 0.87m/s, there is quite a noticeable non-linearity in temperature profiles, which indicates the presence of air motion within
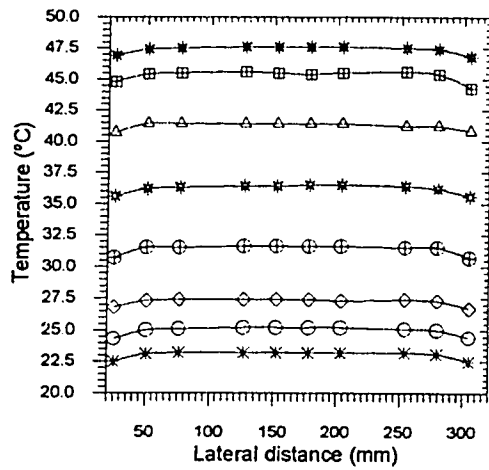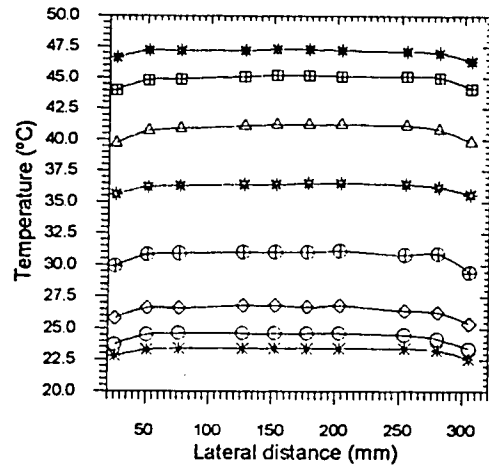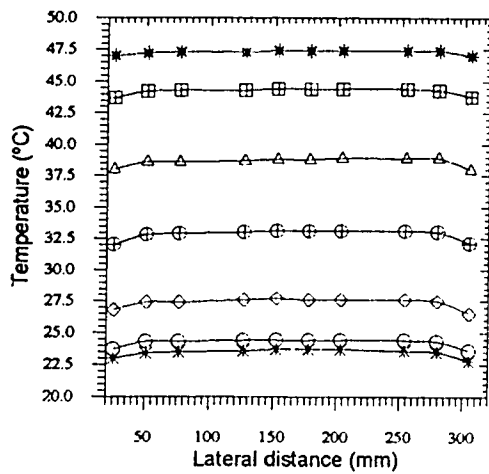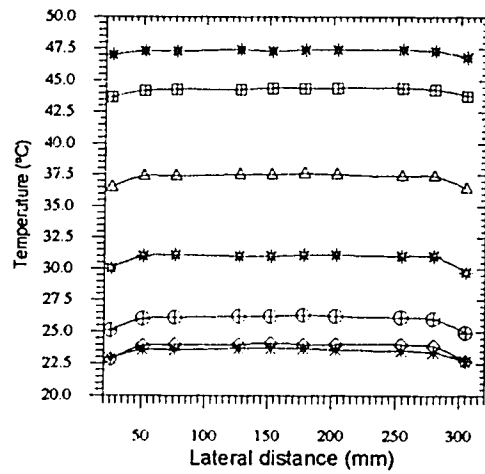
Figure 4.3 *Lateral temperature profiles for the glass fibre insulation sample for different free stream velocities.The plate temperature is 47°C . Measurements taken at 305 mm from the leading edge.*
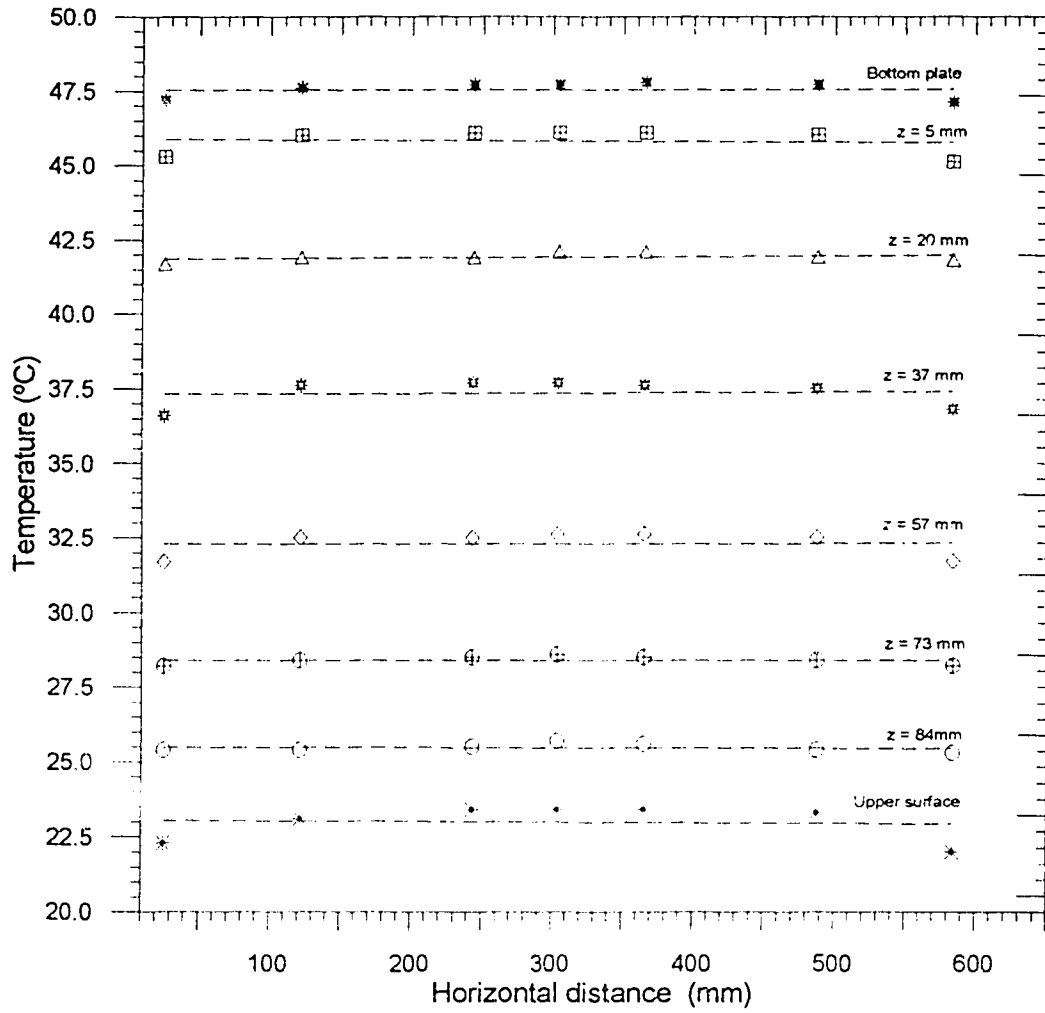
Figure 4.4 *Horizontal temperature profiles for the covered glass fibre insulation sample. The plate temperature is 47°C . Measurements taken along the centre-line.*
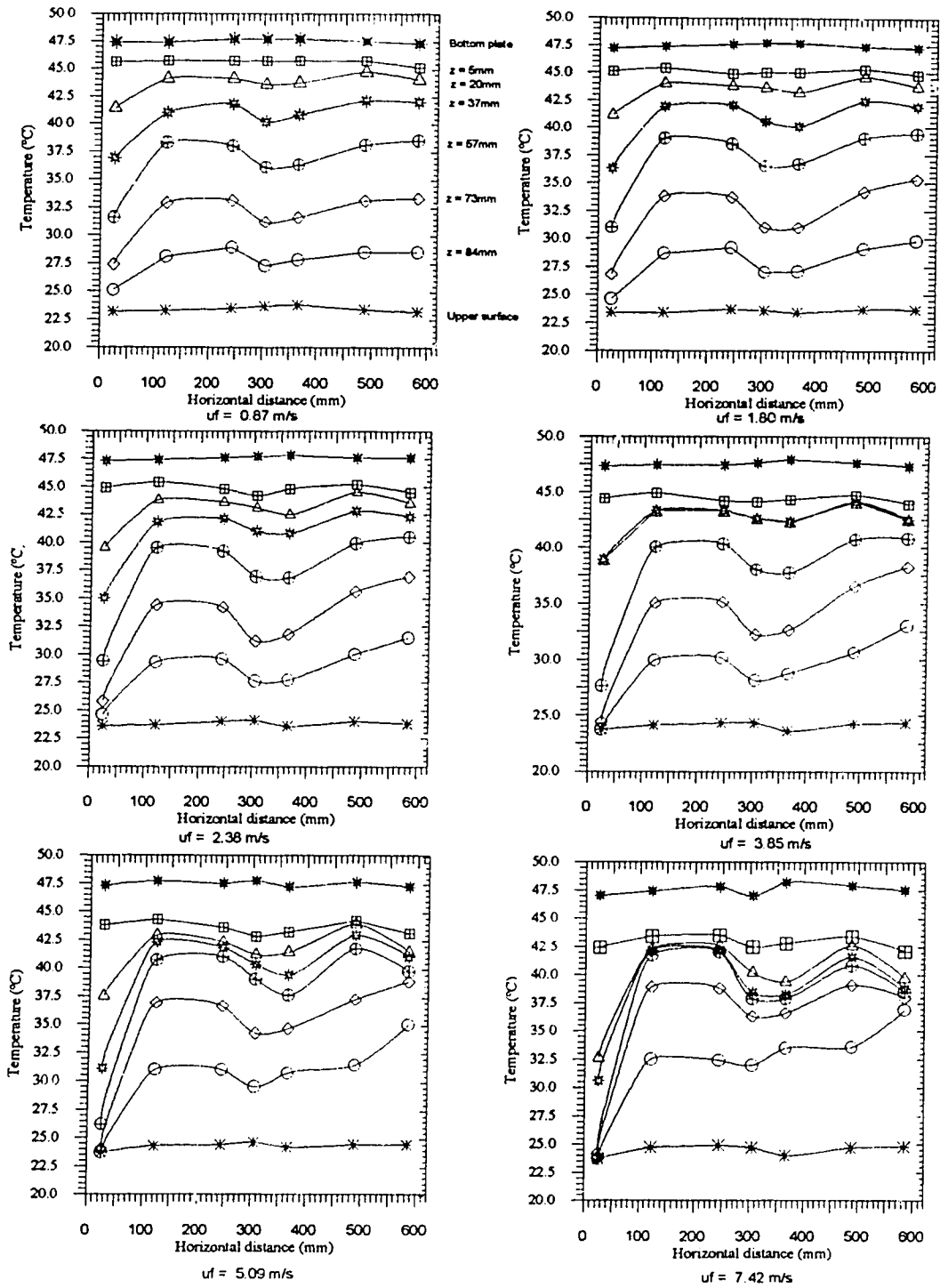
Figure 4.5 *Horizontal temperature profiles measured along the centre-line for different velocities for glass fibre. The plate temperature is 47°C .*

47

the insulation as result of air flow over the surface of the insulation. Similar results are shown in Fig.4.6 and 4.7 for glass fibre for plate temperature of 60°C and 67°C. The implications of these measured temperature profiles will be discussed further in section 4.1.3 once the vertical temperature profiles have been presented.

4.1.3   Vertical temperature variation (z-direction)

Figure 4.8 shows the measured temperature profiles in glass fibre insulation at different locations for a range of air stream velocities from 0.87 to 6.45 m/s with a plate temperature of 47°C. Similarly, Figs. 4.9 and 4.10 present data for plate temperatures 60°C and 67°C respectively. The dotted line in all figures represents the linear best fit to the temperature profile for the insulation sample covered with the aluminum plate. In all covered cases the temperature measurements were very close to linear, indicating that the heat loss was purely by conduction. However, for the case where the aluminum plate was removed, all sets of results clearly show that the temperature profiles deviate significantly from the linear, with a point of inflection about 2 cm from the bottom of the sample. This deviation from the linear profile increases as the free stream velocities increase. Near the top of the sample, the temperature profiles suggest that there was air motion within the insulation in the direction of the stream velocity. These temperature profiles are similar to the temperature profiles presented in Sec 2.2. The fluid shear at the upper surface of the insulation was transmitted to the air within the porous medium and created this motion. On the other hand, near the bottom of the sample the deviation of the temperature profiles was in the opposite direction to the free stream velocity. This would suggest that the induced velocity in this region is in the upstream direction. These results imply some sort of recirculation pattern may be set up within the insulation sample (Fig.4.11). The S-shape temperature profiles were observed for all the locations along the length of the sample. It is interesting to note that at the upstream and downstream ends of the sample, the temperature profiles are similar to those presented in Sec. 2.2(a) indicating that the vertical component of the velocity is more pronounced. However, at intermediate space of the sample, the profiles seem to be a combination of the two cases presented in Secs.
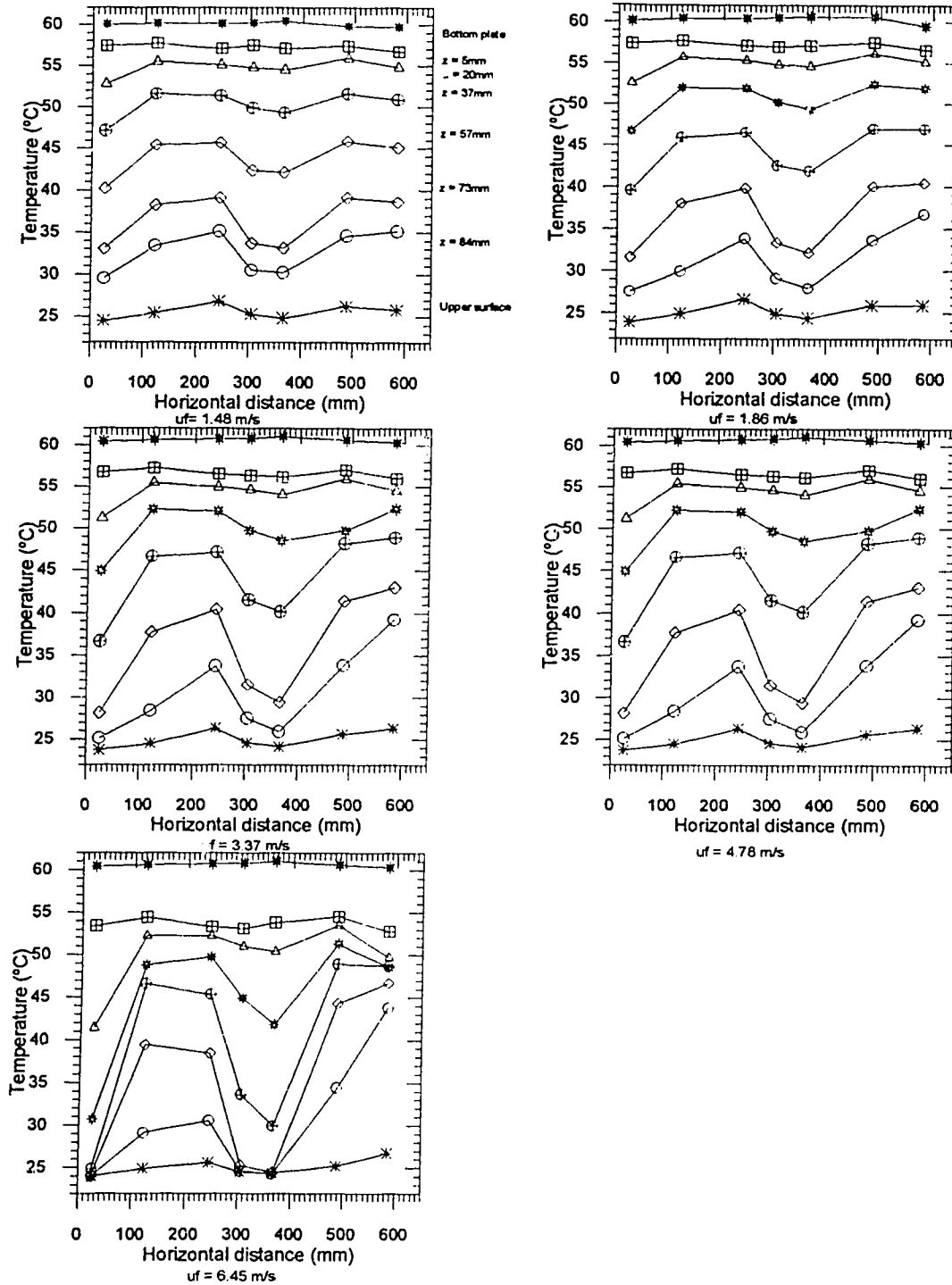
Figure 4.6 *Horizontal temperature profiles measured along the centre-line for different velocities for glass fibre. The plate temperature is 60°C .*
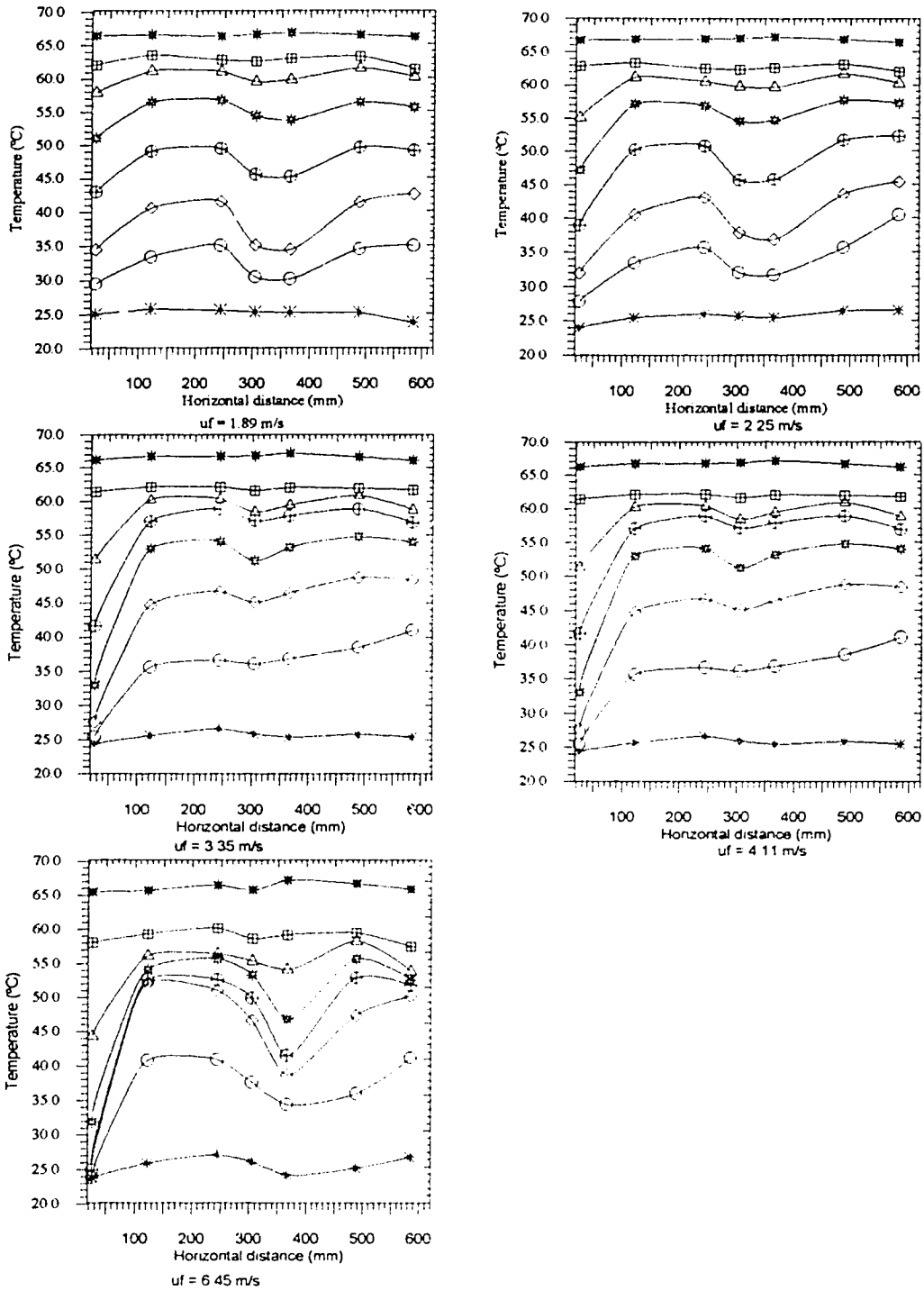
Figure 4.7 *Horizontal temperature profiles measured along the centre-line for different velocities for glass fibre. The plate temperature is 67°C .*
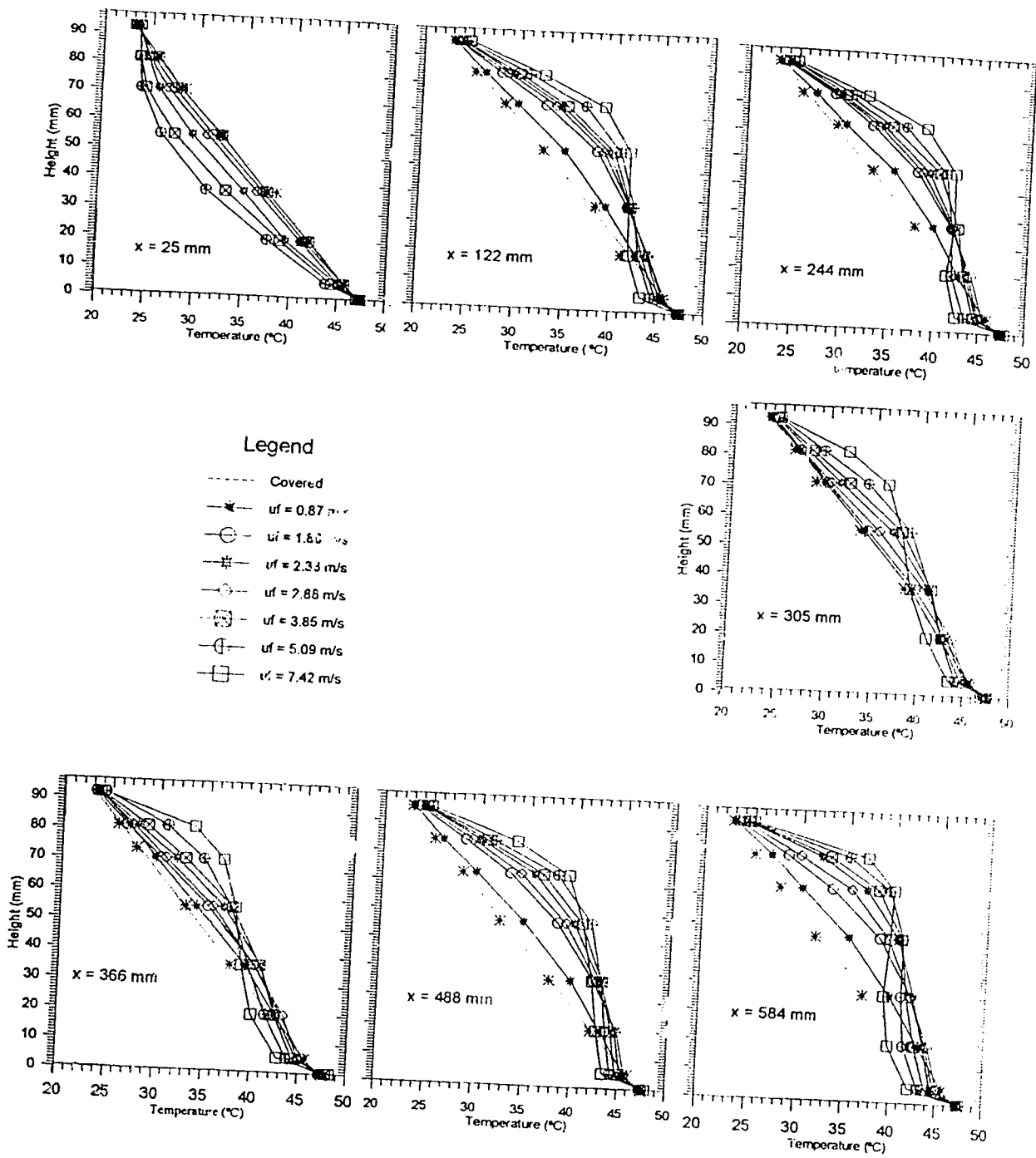
Figure 4.8 *Vertical temperature profiles measured along the centre-line for different velocities for glass fibre. The plate temperature is 47°C.*

51
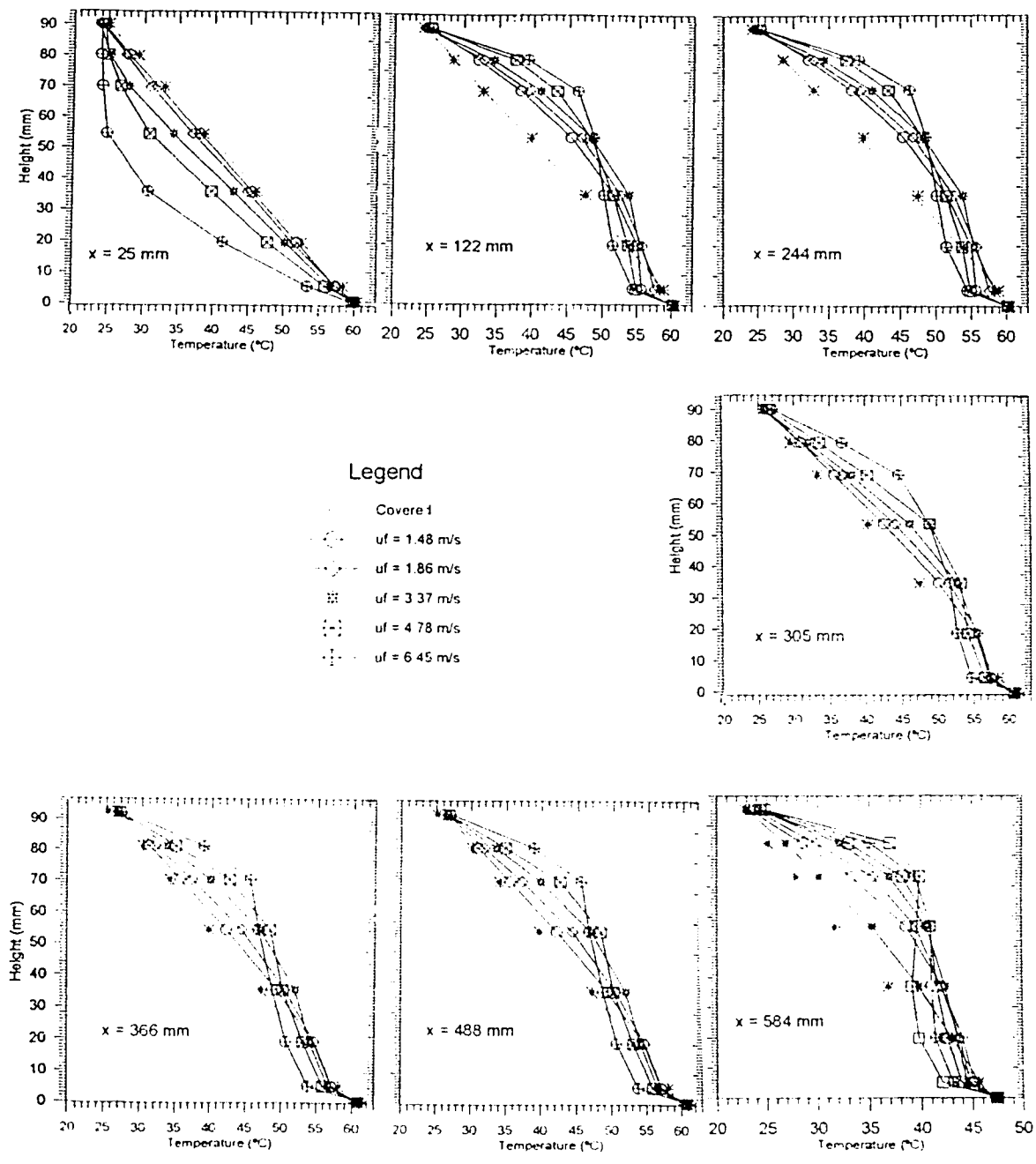
Figure 4.9 *Vertical temperature profiles measured along the centre-line for different velocities for glass fibre. The plate temperature is 60°C .*
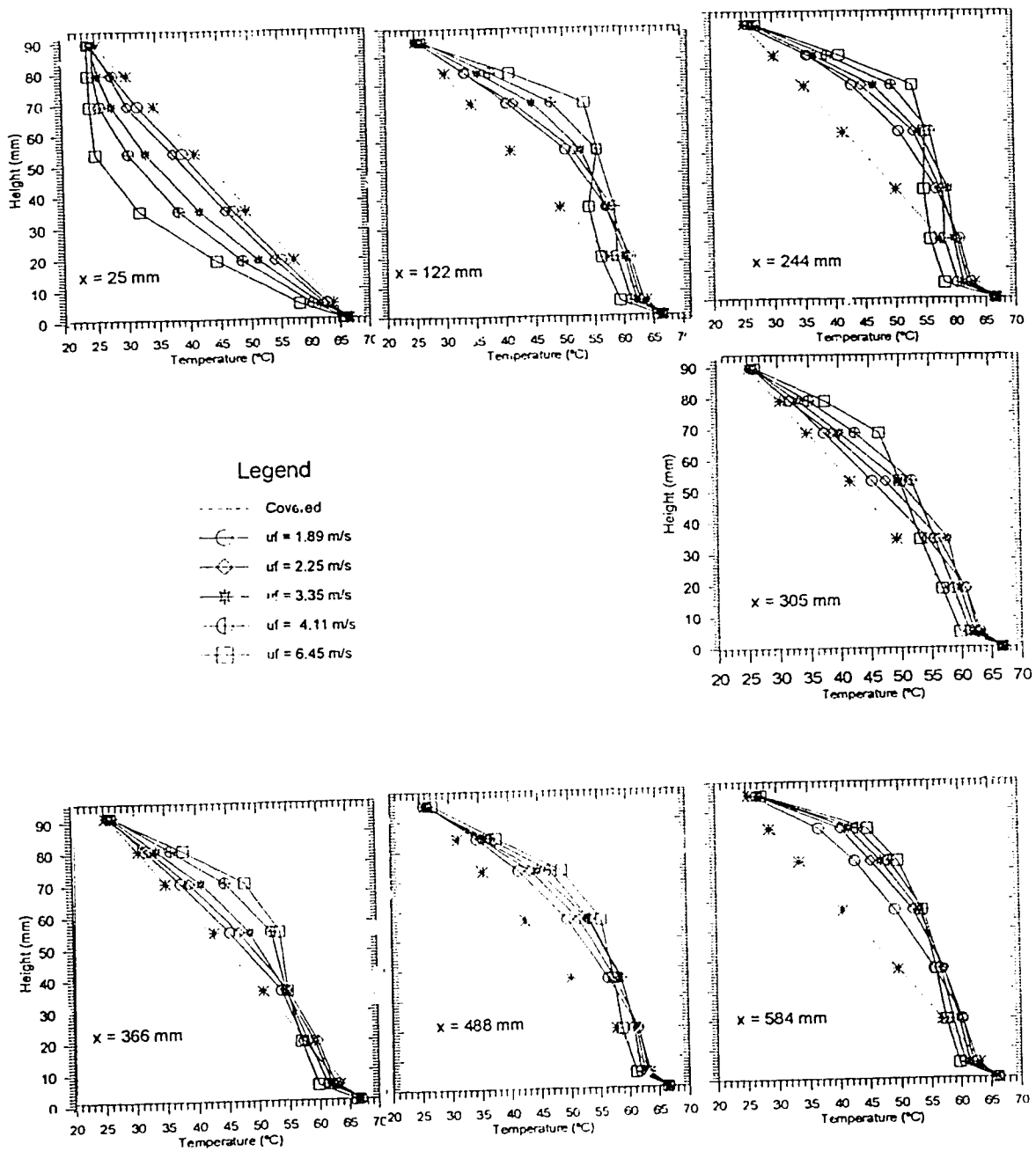
Figure 4.10 *Vertical temperature profiles measured along the centre-line for different velocities for glass fibre. The plate temperature is 67°C .*
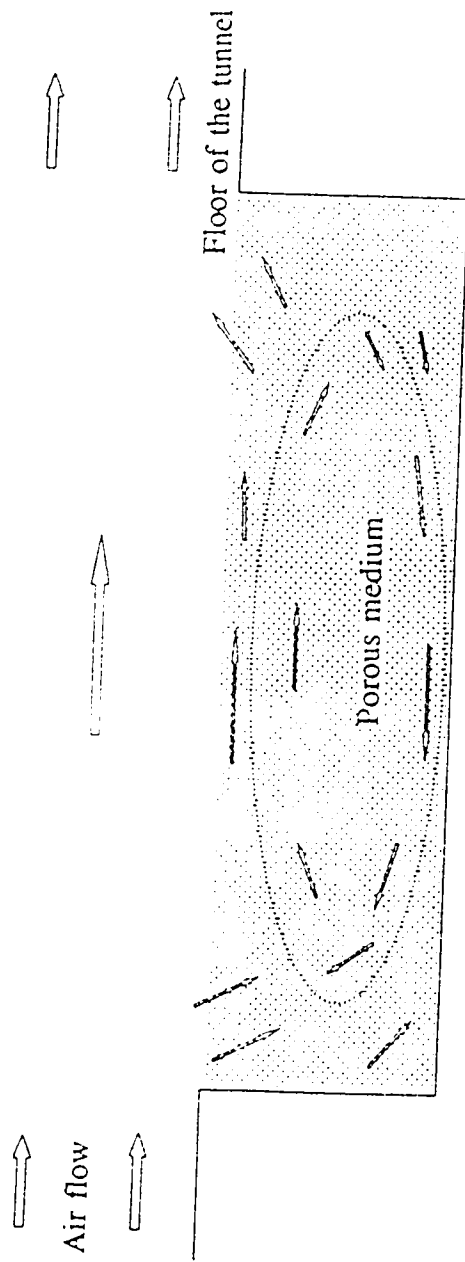
Figure 4.11 *Illustration of air flow within the insulation sample.*

2.2(a) and 2.2(b) indicating some recirculation zone.

4.1.4   Corroboration of measurements

The non-linear temperature profiles shown in the previous figures for the exposed insulation can be corroborated with the measured heat fluxes at different locations. Near the heated plate where air motion is negligible, the heat flux through the insulation can be expressed using Fourier's law of heat conduction;

$$q = -k\frac{\partial T}{\partial z}\Big|_{z=0} \qquad\qquad 4.1$$

The heat flux, q was measured and if the temperature gradient at the heated plate can be estimated from the temperature profiles, then the thermal conductivity of the insulation can be calculated from Eqn.4.1. The value of k should be close to the literature value of 0.0425 W /m.°C for glass fibre insulation (ASHRAE Fundamentals, 1989) and, moreover, the value of k should be independent of the effect of air motion within the sample.

The temperature profiles at the heated plate were estimated by fitting a polynomial of order 4 to the data points. The polynomial was chosen to fit the data near the bottom where the temperature gradient would be calculated. The estimated values of the boundary temperature gradient were calculated using both a fourth and fifth order polynomial fit and there was very little difference (2%) between these estimates. In all subsequent estimates of temperature gradient, a fourth order polynomial fit was used. Results of this analysis for glass fibre insulation are presented in Tables 4.1 to 4.3 for plate temperatures of 47 °C, 60 °C and 67 °C, respectively. In all cases, the estimated values of k varied from 0.044 to 0.049 W/m.°C which is close to the accepted value for glass fibre of 0.042 W/m.°C. The results, also, show that the thermal conductivity is independent of x and the free stream velocity. Thus, the measured temperature profiles are consistent with the measured heat fluxes.

The resistance or "R-Value" for a given thickness of insulation was calculated as

Table 4.1 *Calculated thermal heat conductivity for commercial glass fibre insulation at plate temperature of 47°C.*

u m/s	Measurements taken @ x= 25 mm				Measurements taken @ x= 244 mm			
	Heat loss measured across air gap		$-(\partial T/\partial z)_{z=0}$ °C/m	k W/m.°C	Heat loss measured across the air gap		$-(\partial T/\partial z)_{z=0}$ °C/m	k W/m.°C
	ΔT °C	q W/m²			ΔT °C	q W/m²		
—	1.4	9.1	255.3	0.039	1.8	11.3	256.0	0.044
0.87	1.6	9.9	235.7	0.042	2.0	12.6	280.0	0.045
1.80	1.8	11.3	262.8	0.043	2.4	15.4	317.6	0.045
2.38	2.2	13.7	311.4	0.044	2.7	17.2	346.2	0.047
2.88	2.4	14.9	384.5	0.039	2.8	17.8	370.7	0.048
3.85	3.1	19.8	440.0	0.045	3.2	20.3	424.9	0.048
5.09	3.5	22.6	491.3	0.046	3.9	24.9	509.9	0.049
7.42	4.6	29.1	709.7	0.041	5.4	34.1	731.4	0.046
8.09	5.2	33.2	721.7	0.046	5.9	37.5	833.3	0.045

u m/s	Measurements taken @ x= 365 mm				Measurements taken @ x= 584mm			
	Heat loss measured across the air gap		$-(\partial T/\partial z)_{z=0}$ °C/m	k W/m.°C	Heat loss measured across the air gap		$-(\partial T/\partial z)_{z=0}$ °C/m	k W/m.°C
	ΔT °C	q W/m²			ΔT °C	q W/m²		
—	1.9	12.4	255.8	0.048	1.8	11.4	255.8	0.044
0.87	2.1	13.5	300.0	0.045	2.2	13.6	302.2	0.045
1.80	2.3	14.7	334.1	0.044	2.3	14.1	302.5	0.046
2.38	2.7	17.4	378.7	0.046	2.6	16.5	349.6	0.047
2.88	3.0	18.9	405.5	0.046	2.9	18.3	384.2	0.047
3.85	3.5	22.5	485.3	0.046	3.5	21.9	466.8	0.047
5.09	4.3	26.7	489.1	0.056	4.2	26.4	568.7	0.046
7.42	5.6	34.8	734.3	0.047	5.5	34.4	745.9	0.046
8.09	6.0	37.4	831.1	0.045	6.0	37.8	804.2	0.047

Table 4.2   *Calculated thermal heat conductivity for glass fibre insulation at plate temperature of 60°C.*

u m/s	Measurements taken @ x= 25 mm				Measurements taken @ x= 244 mm			
	Heat loss measured across the air gap		$-(\partial T/\partial z)_{z=0}$ °C/m	k W/m.	Heat loss measured across the air gap		$-(\partial T/\partial z)_{z=0}$ °C/m	k W/m.
	ΔT °C	q W/m²			ΔT °C	q W/m²		
—	2.2	13.6	316.3	0.043	2.9	18.1	365.4	0.049
0.89	2.3	14.3	317.8	0.045	3.1	19.1	406.4	0.047
1.22	2.5	15.8	351.1	0.045	3.2	19.7	410.4	0.048
1.48	2.8	17.3	392.2	0.044	3.2	20.1	441.0	0.045
1.86	2.9	18.2	433.3	0.042	3.6	22.3	469.3	0.047
3.37	3.9	24.4	546.8	0.045	4.5	28.0	584.6	0.048
4.78	4.3	26.9	661.9	0.041	5.0	31.5	642.9	0.049
5.14	5.3	33.4	776.7	0.043	6.4	39.8	904.5	0.044
6.45	6.6	41.3	969.0	0.043	8.0	50.2	966.1	0.049

u m/s	Measurements taken at x= 365 mm				Measurements taken @ x = 584mm			
	Heat loss measured across the air gap		$-(\partial T/\partial z)_{z=0}$ (°C/m)	k (W/m.°C)	Heat loss measured across the air gap		$(\partial T/\partial z)_{z=0}$ °C/m	k W/m.°C
	ΔT °C	q W/m²			ΔT °C	q W/m²		
—	2.9	18.1	365.1	0.049	3.2	20.1	410.2	0.049
0.89	3.0	19.0	387.8	0.049	3.2	20.1	404.0	0.050
1.22	3.2	20.2	420.8	0.048	3.3	20.4	416.3	0.049
1.48	3.4	21.5	438.8	0.049	3.3	20.4	424.5	0.049
1.86	3.6	22.7	434.8	0.047	3.5	21.7	442.8	0.049
3.37	4.7	29.3	609.5	0.048	4.5	28.0	570.3	0.049
4.78	5.1	31.8	658.6	0.048	4.9	30.8	630.4	0.049
5.14	6.2	38.5	819.1	0.047	6.0	37.6	800.0	0.047
6.45	7.1	48.6	^95.1	0.049	7.7	48.3	1005.5	0.048

Table 4.3   *Calculated thermal heat conductivity for glass fibre insulation at plate temperature of 67°C.*

u m/s	Measurements taken @ x= 25 mm				Measurements taken @ 244 mm			
	Heat loss measured across the air gap		$-(\partial T/\partial z)_{z=0}$ °C/m	k W/m.°C	Heat loss measured across the air gap		$-(\partial T/\partial z)_{z=0}$ °C/m	k W/m.°C
	ΔT °C	q W/m²			ΔT °C	q W/m²		
---	2.8	17.5	422.3	0.041	3.4	21.3	490.1	0.044
0.95	3.0	18.6	442.9	0.042	3.5	22.0	478.3	0.046
1.89	3.5	21.6	534.4	0.040	3.7	23.2	487.9	0.047
2.25	4.2	26.2	630.7	0.041	4.7	29.5	594.4	0.049
2.65	4.3	27.1	655.7	0.041	4.9	30.6	612.6	0.049
3.35	5.2	32.3	781.5	0.041	5.9	37.1	789.4	0.047
4.11	5.8	36.1	885.1	0.041	6.7	41.6	843.9	0.047
5.55	6.6	41.5	922.2	0.045	7.6	47.8	1062.2	0.045
6.45	7.9	49.1	1115.9	0.044	8.9	55.8	1079.8	0.042

u m/s	Measurements taken @ x = 365mm				Measurements taken @ x= 584 mm			
	Heat loss measured across the air gap		$-(\partial T/\partial z)_{z=0}$ °C/m	k W/m.°C	Heat loss measured across the air gap		$-(\partial T/\partial z)_{z=0}$ °C/m	k W/m.°C
	ΔT °C	q W/m²			ΔT °C	q W/m²		
----	3.6	22.5	459.2	0.049	3.3	20.7	422.3	0.049
0.95	3.7	23.4	497.9	0.047	3.7	22.9	487.2	0.047
1.89	4.2	26.1	553.8	0.047	3.9	24.6	511.4	0.048
2.25	4.9	30.7	636.2	0.048	4.7	29.2	595.9	0.049
2.65	5.2	32.2	663.6	0.048	5.0	31.0	632.6	0.049
3.35	6.0	37.7	771.3	0.049	5.8	36.5	744.9	0.049
4.11	7.1	44.2	851.4	0.049	6.6	41.2	840.8	0.049
5.55	7.9	49.1	1022.9	0.048	7.8	48.?	1086.7	0.045
6.45	9.1	56.7	1148.6	0.049	9.0	56.4	1226.1	0.046

the ratio of the temperature difference sample over the heat flux across the insulation sample;

$$R = \frac{\Delta T}{q} \qquad\qquad 4.2$$

At each of the different velocities, these R-values should be interpreted as "effective" R-values since the definition in Eqn 4.2 is based on pure conduction. Table 4.4 gives the "effective" R-values for the three plate temperatures. The values based on the covered samples reflect the true R-value for the insulation and are very close to standard R-values quoted for glass fibre insulation. However, for the exposed insulation at different air velocities, the effective R-values are significantly less than the standard value. The loss in insulating property can be significant with a reduction by a factor of 3 to 4 for air velocity on the order 6 to 7 m/s.

4.2 Effect of Permeability

The permeability as discussed in Chapter 2 is a measure of the resistance of the porous media to flow. In the present case, changing permeability should change the heat loss through the sample. Increasing the permeability should increase the amount of air intrusion into the sample and cause an increase in heat loss; conversely, decreasing permeability should decrease the heat loss by restricting air intrusion in the insulation sample. A set of tests was carried out using a glass fibre furnace filter material and compressing it to different densities to achieve different permeabilities.

Horizontal and vertical temperature profiles are shown in Figs 4.12 (a) and 4.12(b), and Figs. 4.13 (a) and 4.13(b) respectively for two selected values of K of 2.49 x 10⁻⁸ m² and 7.62 x 10⁻⁸ m². Tests at intermediate values of K were conducted but the results are not presented here. In each case, the measured temperature profiles are similar to those shown for the glass fibre sample, except that the effect of the free stream velocity is more pronounced. For example at the inlet (x = 25 mm) the vertical temperature

Table 4.4 *Effective R-values for commercial glass fibre insulation.*

Temperature : 47°C		Temperature : 60°C		Temperature : 67°C	
Velocity (m/s)	R-value (m².°C/W)	Velocity (m/s)	R-value (m².°C/W)	Velocity (m/s)	R-value (m².°C/W)
----	2.06	----	2.01	----	1.97
0.87	1.94	0.89	1.92	0.95	1.88
1.80	1.67	1.22	1.71	1.89	1.58
2.38	1.55	1.48	1.62	2.25	1.29
2.88	1.39	1.86	1.51	2.65	1.22
3.85	1.09	3.37	1.19	3.35	1.02
5.09	0.88	4.78	0.9	4.11	0.86
7.42	0.64	5.14	0.77	5.55	0.72
9.09	0.50	6.45	0.60	6.45	0.61
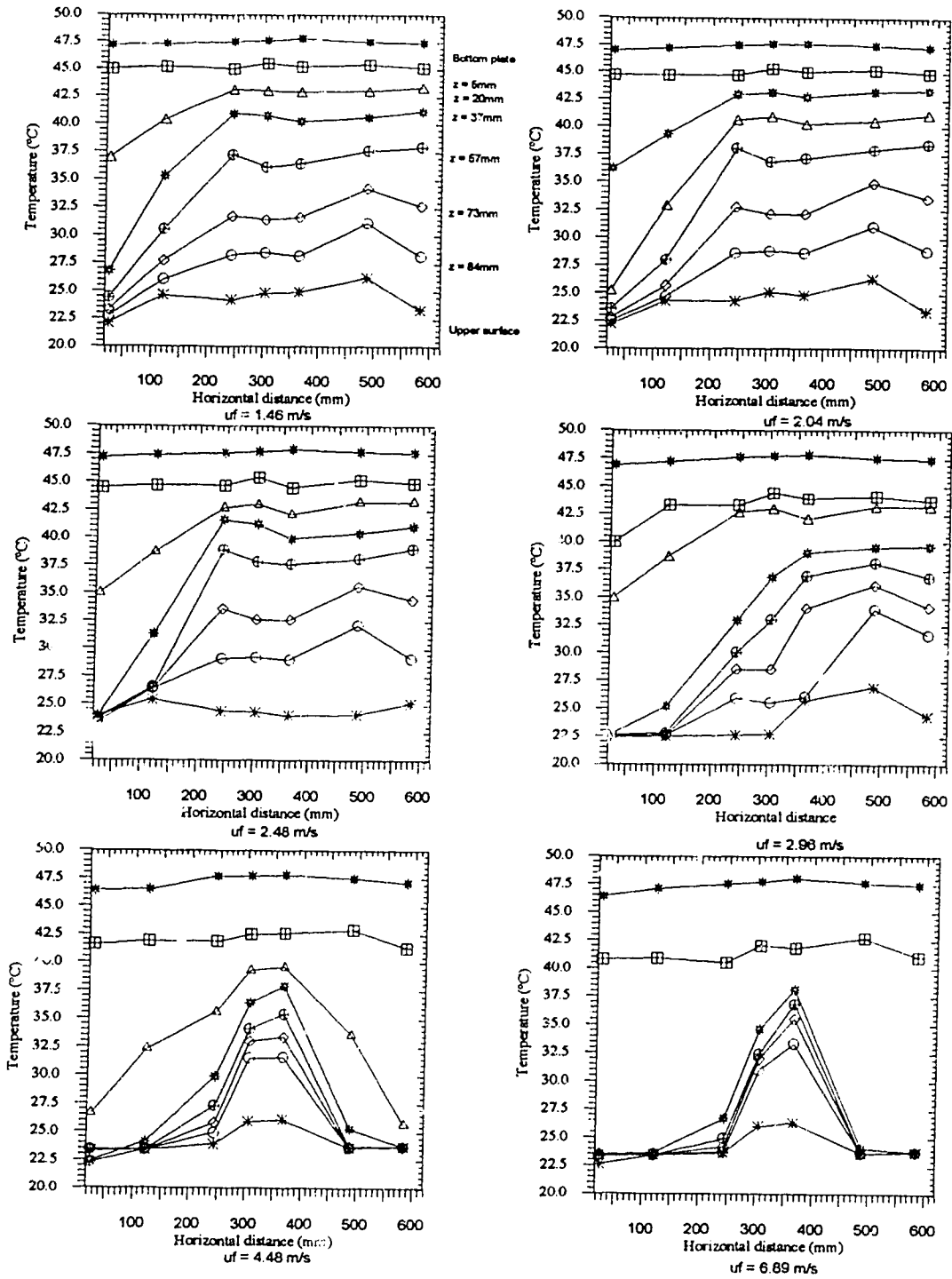
Figure 4.12(a) *Horizontal temperature profiles for different velocities for glass fibre. The permeability, K, is 2.49 x 10⁻⁸ m².*

61

Figure 4.12(b) *Vertical temperature profiles measured along the centre-line for different velocities for glass fibre furnace filter material. The permeability, K, is $2.49 \times 10^{-8}\, m^2$.*

Figure 4.13(a) *Horizontal temperature profiles for different velocities for glass fibre. The permeability, K, is 7.62 x 10⁻⁸ m².*
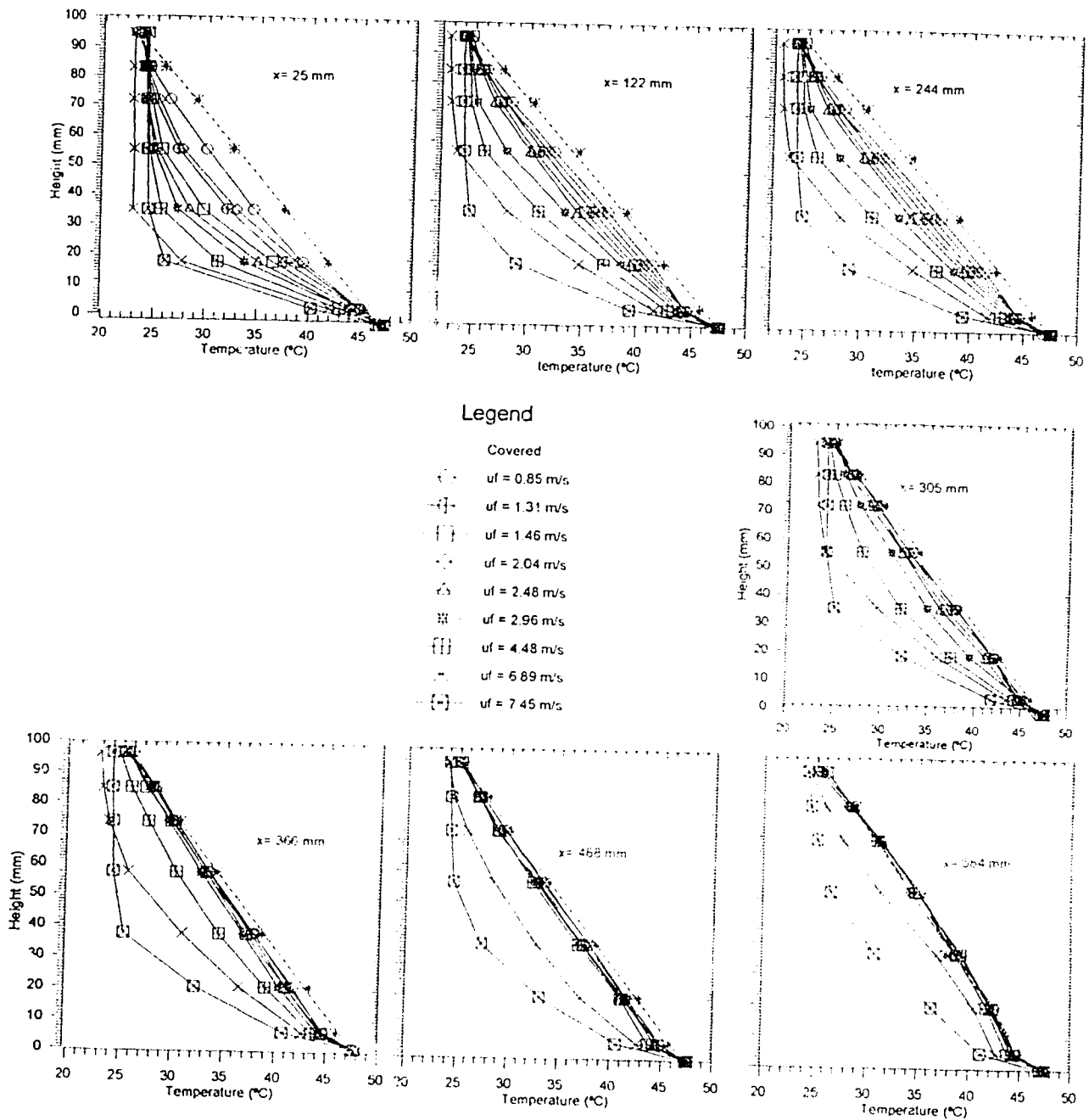
63

Figure 4.13(b) *Vertical temperature profiles measured along the centre-line for different velocities for glass fibre furnace filter material. The permeability, K, is 7.62 x 10⁻⁸ m².*
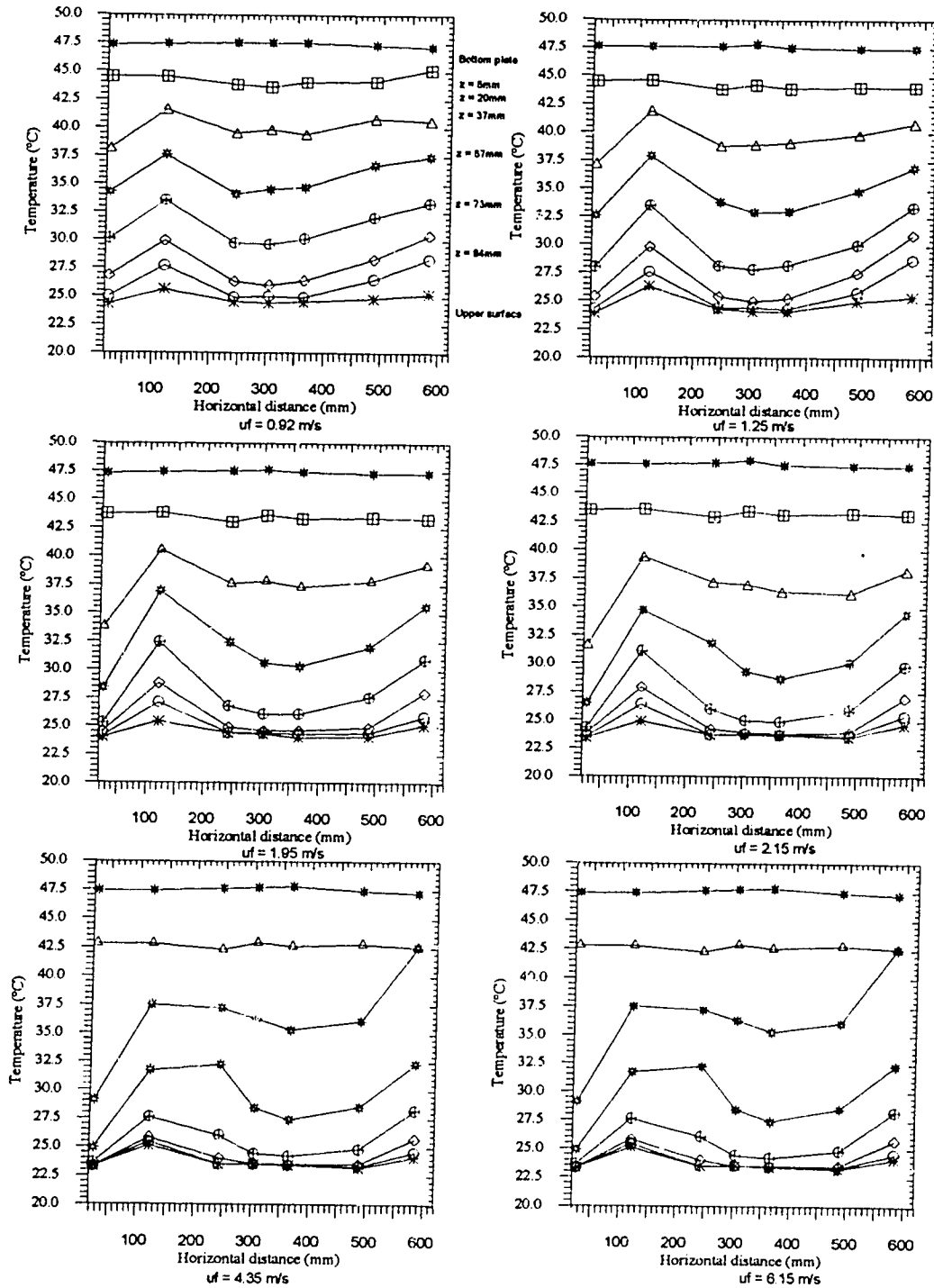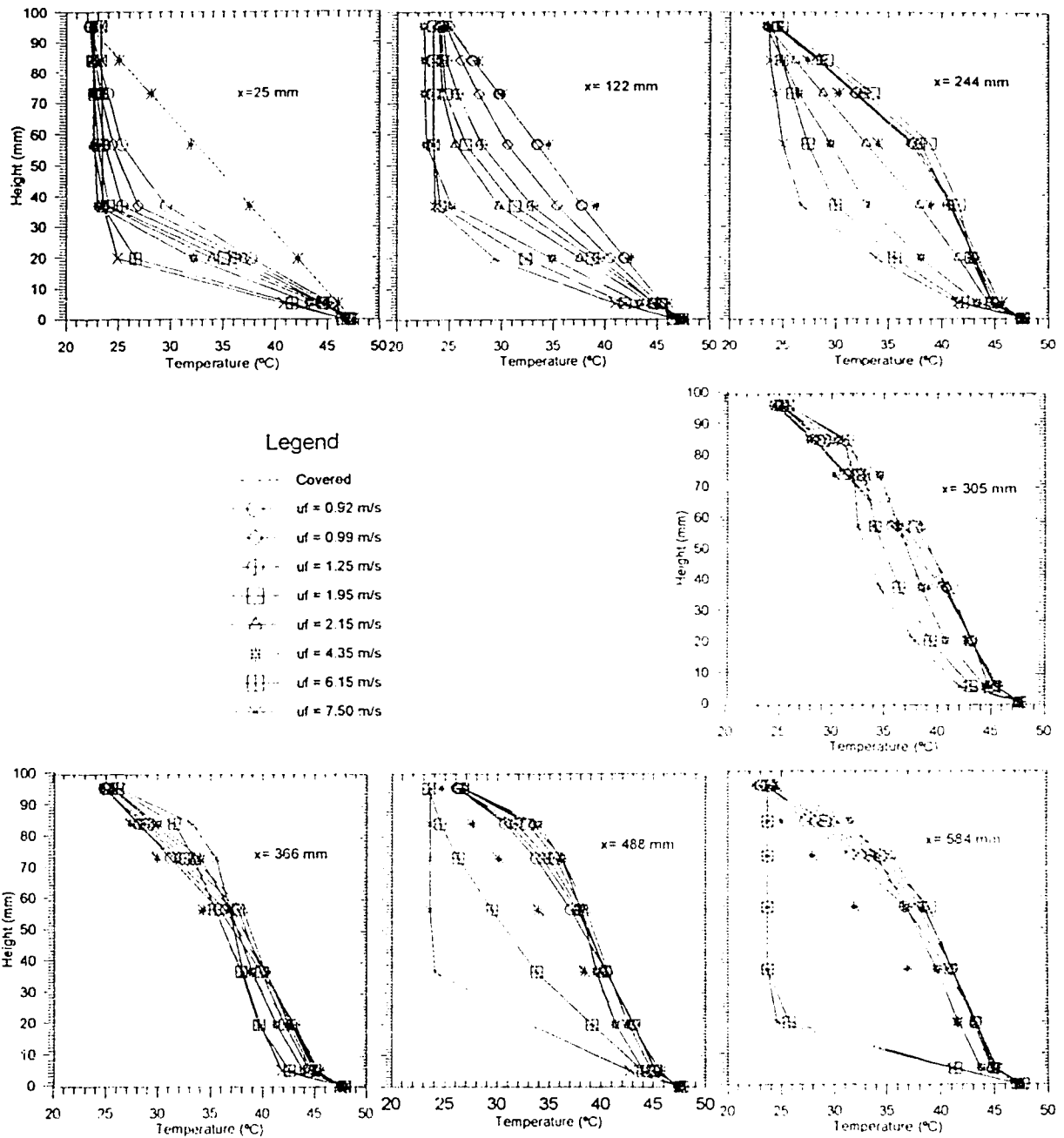
profiles, shown in Fig. 4.12(b) indicate a large downward z component of velocity which keeps the temperature constant at ?1 °C approximately 2/3 of the way down through insulation. This is not unexpected since the permeability of the sample is 7.62×10^{-8} m^2 which is almost 1 order of magnitude larger than the glass fibre sample. It is interesting to note that the temperature profiles for the high permeability insulation do not exhibit an inflection as did the glass fibre temperature profiles shown in Figs 4.8 to 4.10.

The values of the thermal conductivity were estimated using the same procedures as outlined above and these results are shown in Tables 4.5 to 4.11. For each permeability, the thermal conductivities were independent of x and u$_f$ (free stream velocity) but the value did change for different permeabilities. For higher permeabilities, k should approach the value for air (0.026 W/m.°C, Holman, 1963) at room temperature. For the largest permeability tested (K= 7.62×10^{-8} m^2), the thermal conductivity is 0.036 W/ m.°C, while for the lowest permeability of glass fibre furnace filter tested (2.49 x 10^{-8} m^2) k $\approx$ 0.036 W/ m.°C. The inferred k values are shown in Fig.4.14 as a function of K.

The corresponding R-values for the glass furnace filter sample are given in Fig.4.15. For a given air flow velocity, R-values increase with increasing permeability due to the decrease in thermal conductivity as K increases. But at the highest permeability tested, the effective R-value is very sensitive to the effects of air intrusion and decreases rapidly with increasing air flow velocity. This effect is not as dramatic for the lowest permeability tested.

4.3 Nusselt Number Correlation

A summary of the measured results can be presented in the usual form of a correlation between the Nusselt number and the Reynolds number for the effect of the flow velocity on heat transfer through insulation. The effect of the permeability on heat transfer can be expressed in terms of the Darcy number which is defined as

Table 4.5 *Calculated thermal conductivity for glass fibre furnace filter. Permeability is 2.49 x 10^{-8} m^2.*

Velocity (m/s)	Measurements taken @ location x = 305 mm			
	Heat loss measured across the air gap		$-(\partial T/\partial z)_{z=0}$ (°C/m)	k (W/m.°C)
	ΔT (°C)	q (W/m^2)		
---	1.6	10.5	269.2	0.039
1.31	1.8	11.3	289.7	0.039
1.46	1.9	12.5	312.5	0.040
2.04	2.0	13.1	327.5	0.040
2.48	2.1	13.6	331.7	0.041
2.96	2.2	14.1	335.7	0.042
4.48	2.6	16.7	407.3	0.041
6.89	3.0	19.4	485.0	0.040
7.45	3.2	20.6	515.0	0.040

Table 4.6 *Calculated thermal conductivity for glass fibre furnace filter. Permeability is 2.74 x 10^{-8} m^2.*

| Velocity (m/s) | Measurements taken @ location x = 305 mm | | | |
| | Heat loss measured across the air gap | | $-(\partial T/\partial z)_{z=0}$ (°C/m) | k (W/m.°C) |
	ΔT (°C)	q (W/m²)		
---	1.4	9.2	255.6	0.036
0.88	1.5	9.3	258.3	0.036
1.46	1.6	9.9	260.5	0.038
2.04	1.7	10.5	283.8	0.037
2.48	1.8	11.6	341.2	0.034
2.97	1.9	12.1	355.9	0.034
4.48	2.1	13.4	372.2	0.036
6.89	2.8	17.6	488.9	0.036
7.56	3.4	21.5	565.8	0.038

Table 4.7 *Calculated heat conductivity for glass fibre furnace filter. Permeability is 3.42 x 10⁻⁸ m².*

Velocity (m/s)	Measurements taken @ location x = 305 mm			
	Heat loss measured across the air gap		$-(\partial T/\partial z)_{z=0}$ (°C/m)	k (W/m.°C)
	ΔT (°C)	q (W/m²)		
---	1.3	8.6	245.7	0.035
0.91	1.4	8.8	251.4	0.035
1.21	1.5	9.2	255.6	0.036
1.95	1.7	10.7	297.2	0.036
2.45	2.0	12.7	362.9	0.035
3.16	2.:	13.4	372.2	0.036
4.85	2.3	14.7	432.3	0.034
5.76	2.5	15.9	441.7	0.036
7.80	2.9	18.5	5:⸱(	0.035

Table 4.8 *Calculated thermal conductivity glass fibre furnace filter. Permeability is 4.22 x 10⁻⁸ m².*

Velocity (m/s)	Measurements taken @ location x = 305 mm			
	Heat loss measured across the air gap		$-(d\partial/\partial z)_z$ (°C/m)	k (W/m.°C)
	ΔT (°C)	q (W/m²)		
---	1.3	8.2	241.2	0.034
0.80	1.4	8.4	240.0	0.035
1.40	1.5	8.9	261.8	0.. 4
1.88	1.6	9.7	285.3	0.034
2.45	1.7	10.6	321.2	0.033
3.06	1.8	1! 5	338.2	0.036
5.06	2.0	12.8	376.5	0.034
5.19	2.5	16.2	450.0	0.036
8.66	2.7	17.4	411.8	0.034

Table 4.9 Calcula. d c ermal heat conductivity for glass fibre furnace filter.
Perm.   . : 5.56 x 10⁻ m².

Velocity (m/s)	Measurements taken @ location x = 305 mm			
	Heat loss measured across the air gap		$-(\partial T/\partial z)_{z=0}$ (°C/m)	k (W/m.°C)
	ΔT (°C)	q (W/m²)		
---	1.0	6.4	206.4	0.031
0.89	1.2	7.8	236.4	0.032
1.12	1.4	8.8	266.7	0.033
1.42	1.7	10.6	331.2	0.032
1.85	1.8	11.7	354.5	0.033
1.87	2.0	12.5	357.1	0.035
2.36	2.2	13.3	403.0	0.033
4.13	2.3	13.8	404.9	0.034
6.15	2.4	14.6	442.4	0.033

Table 4.10 *Calculated thermal heat conductivity for g…ss fibrefurnace filter.*
Permeability is 6.63 x 10⁻⁸ m².

| Velocity (m/s) | Measurements taken @ location x = 305 mm | | | |
| | Heat loss measured across the air gap | | $(\partial T/\partial z)_{z=0}$ (°C/m) | k (W/m.°C) |
	ΔT (°C)	(W/m²)		
---	0.9	6.2	213.8	0.029
0.95	1.0	6.3	217.2	0.029
1.50	1.1	7.3	243.3	0.030
2.10	1.4	8.7	280.6	0.030
2.75	1.5	9.3	290.6	0.031
3.75	1.6	9.7	303.6	0.032
4.27	1.7	10.3	312.8	0.032
5.14	1.8	11.1	382.8	0.029
6.38	1.9	12.2	420.7	0.029

Table 4.1) *ulated thermal heat conducti·ity i· glass fibre furnace fi!t·r. Per ·eability is 7.62 x 10⁻⁶ m².*

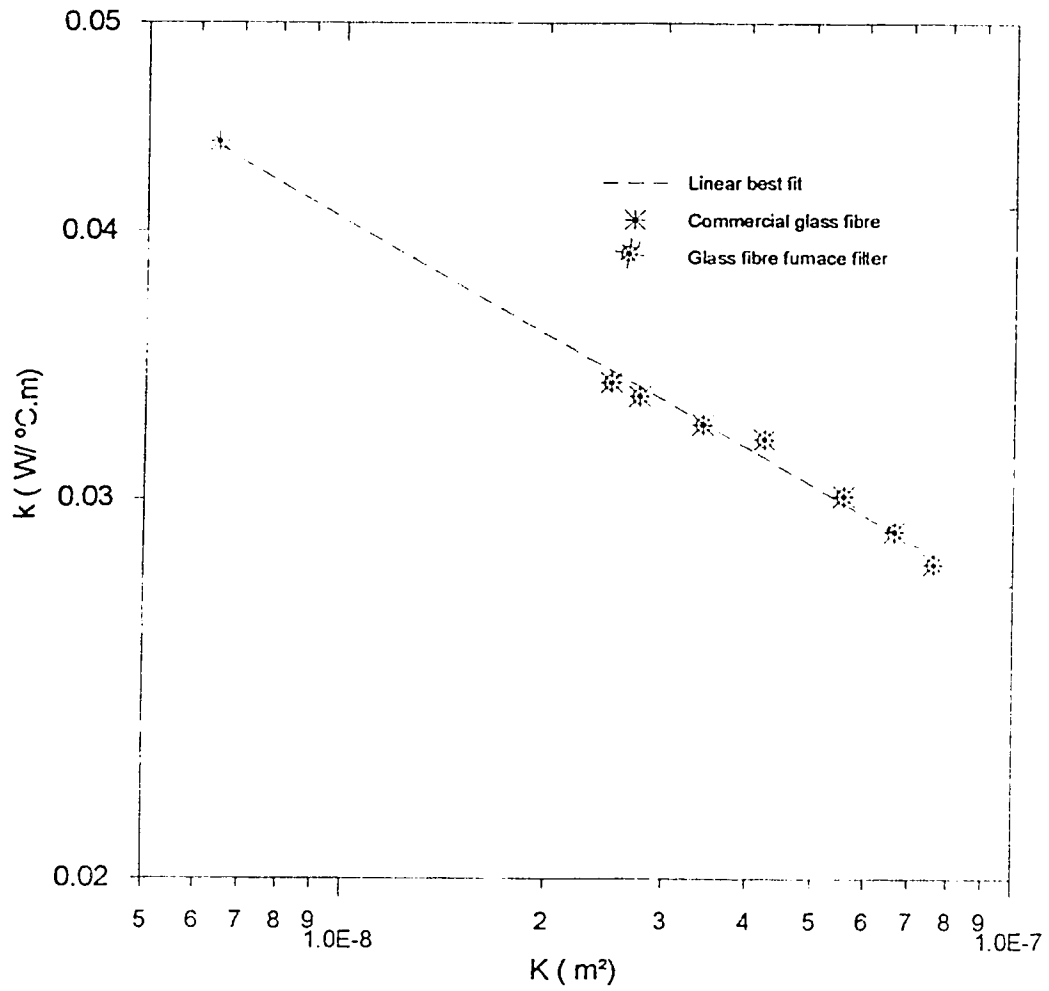| Velocity (m/s)	Measurements taken @ location x = 305 mm			
	Heat loss measured across the air gap		$-(\partial T/\partial z)_{z=0}$ (°C/m)	k (W/m.°C)
	ΔT (°C)	q (W/m²)		
---	0.8	5.6	214.8	0.028
0.92	0.9	5.9	217.9	0.027
0.99	1.0	6.1	230.0	0.028
1.25	1.1	6.9	243.3	0.030
1.95	1.2	7.3	270.0	0.030
2.15	1.3	8.1	355.2	0.030
4.35	1.6	10.3	417.9	0.029
6.15	1.8	11.7	424.2	0.028
7.50	1.9	12.3	424.2	0.028

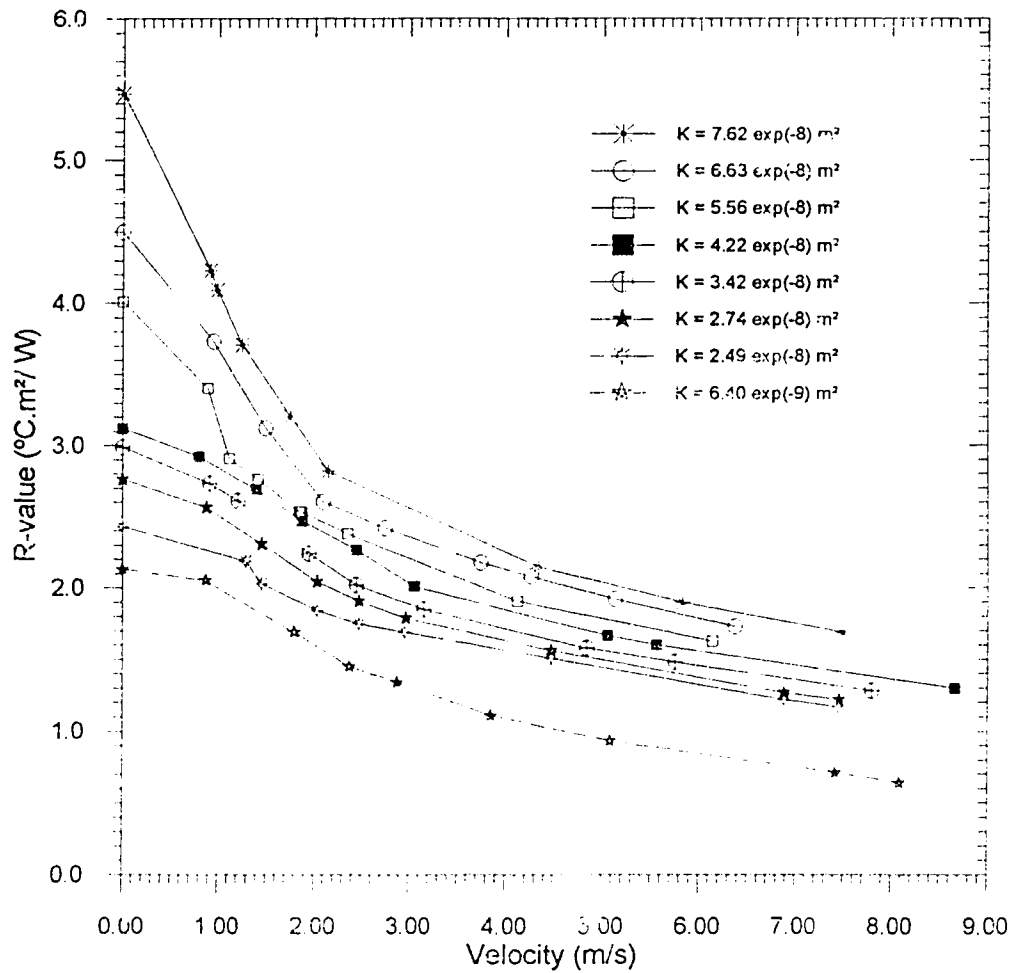**Figure 4.14**   *Thermal heat conductivity for different permeabilities.*

Figure 4.15 *Effect of the free stream velocity on the R-value for different permeabilities; the continuous lines are for glass fibre furnace filter material, and the dashed line is for glass fibre.*

$$Da = \frac{K}{a^2} \qquad\qquad 4.3$$

where a is the mean fibre diameter. Dimensional analysis on the basic variables involved in the problem indicates a relationship of the form (Dybbs *et al*, 1986)

$$f(\ Nu,\ Re,\ Da) = 0 \qquad\qquad 4.4$$

where Nu is the heat conduction-based Nusselt number defined as the ratio of the average measured heat flux, q, over the average heat flux, q_{cond}, which is measured when the sample is covered with the aluminum plate:

$$Nu = \frac{q}{q_{cond}}$$

The Reynolds number, Re is defined as

$$Re = \frac{u_f\ L}{v}$$

In the present case, Re is based on the free stream velocity, u_f, and the length of the insulation sample, L. For these tests the length of the insulation sample is 610 mm. Figure 4.16 shows the measured Nu-Re for the case of glass fibre for three different plate temperatures. These results are independent of plate temperature over the range tested, and provide an additional corroboration of the measurements. Using a linear best fit to the data of Fig. 4.16 , Nu-Re correlation would be a power law correlation;
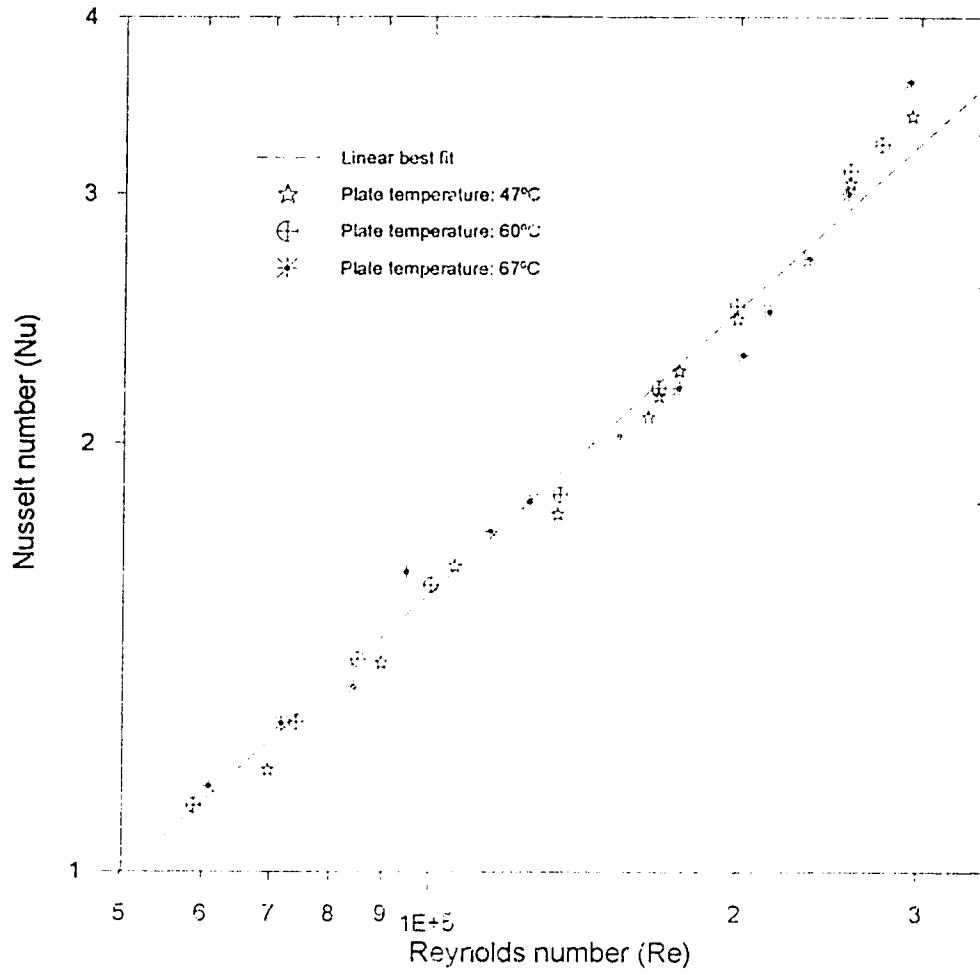
Figure 4.16 *Nu - Re correlation for glass fibre for different plate temperatures.*
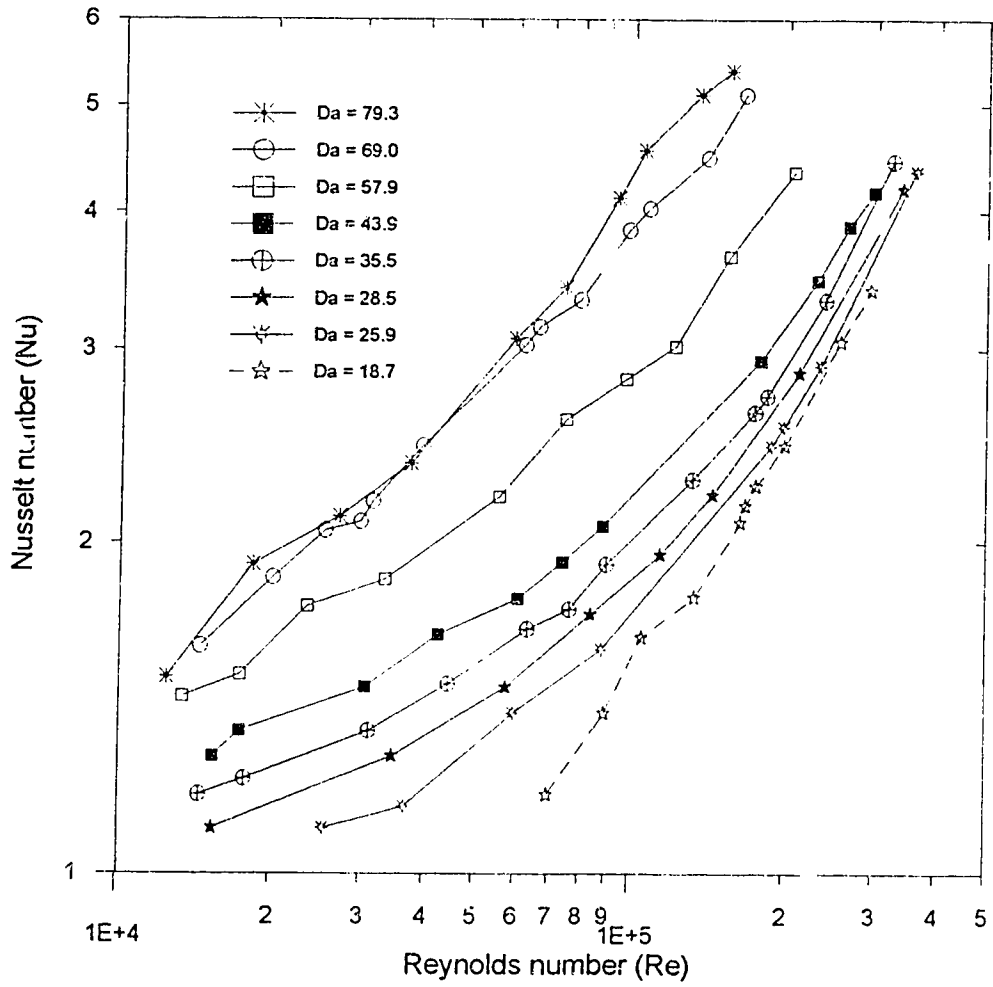
Figure 4.17 *Nu - Re correlation for different permeabilities for different values of Darcy number; the continuous lines are for glass fibre furnace filter material, and the dashed line is for glass fibre.*
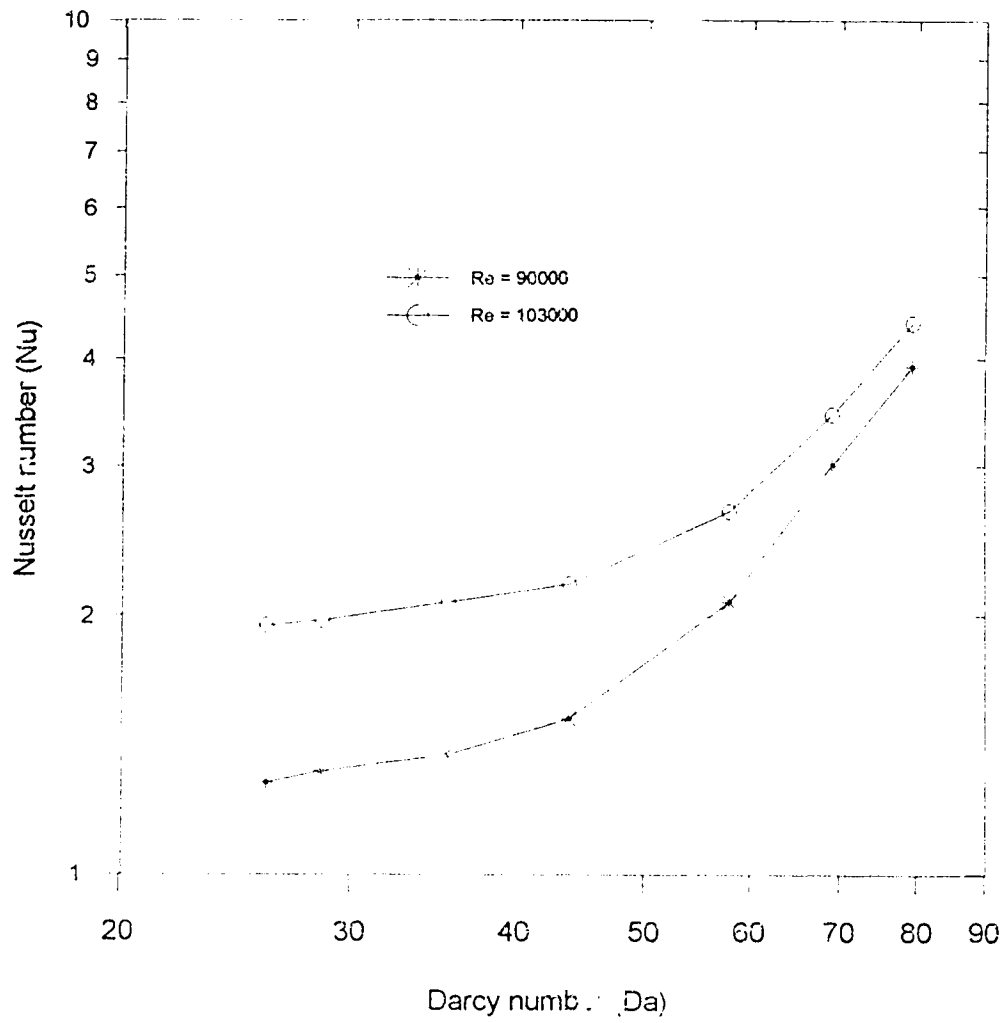
Figure 4.18 *Nu - Da correlation Re for different permeabilities.*

$$Nu = C\ Re^{0.6?} \qquad\qquad 4.5$$

where C is a constant. Figure 4.17 shows the Nu-Re for glass fibre furnace filter material for different Darcy numbers. Figure 4.18 shows the Nu-Da correlation for 2 values of Reynolds number. At each Darcy number, the Nusselt number increases significantly over the range tested. The largest change in Nu occurs for the insulation with the largest Darcy number. This simply reflects the very open structure of the insulation and its low resistance to air intrusion.

CONCLUSIONS AND RECOMMENDATIONS

An experimental study was conducted to investigate systematically the effect of air flow over an exposed surface on heat transfer through porous insulation. Glass fibre based porous insulation was tested for a range of permeabilities of 2×10^{-8} m^2 to 5×10^{-9} m^2, the latter limit corresponding to c mercial glass fibre insulation.

This study showed that heat transfer through porous insulation can be increased significantly by air flow over an exposed surface of the sample. This has implications for the use of this type of insulation in certain areas of building envelopes. Intrusive air flow serves to degrade the R-value of porous insulation sample. A permeable insulator sealed on all sides except one could have its effective R-value degraded by forced air flow coupled at its unsealed surface. The data presented here appear to indicate that the air flow over the surface of a permeable material induces flow within the porous medium. The temperature profiles suggest that there was air movement within the insulation in the direction of the free stream velocity. The fluid shear at the upper surface of the insulation was transmitted to the air within the porous medium and created this motion. The net result was that the heat loss through the sample increased as the free stream velocity increased. For the range of conditions tested, the relative effect of air velocity on enhancement of heat flux was independent of the temperature difference across the sample. These results showed that the R-values of the porous insulation can be reduced by a factor of 2 to 3 for a moderate air flow over the surface of the insulation up to 9 m/s.

5.1   Conclusions

1- Air flow over surface increases the heat flux by creating forced convective motion within the insulation. For velocity up to 9 m/s the heat flux increases by a factor of approximately 3. Effective R-values for glass fibre insulation changes by a factor of 2 to 3 for a range of velocity from 0 to 9 m/s.

2- High permeable insulation has low thermal conductivity (close to that of air) and therefore high R-value. But heat flux is very sensitive to effects of air intrusion. Effective R-value changes from 6 to 2 °C m^2/W for velocities up to 7 m/s while the lowest permeable insulation tested had R-value from 2 to 5. These results suggest using lower density insulation in buildings.

5.2   Recommendations for Further Studies

For further analysis, tests should be repeated in a larger cross section wind tunnel where the expansion in flow area is small compared to the cross-section of the tunnel. Furthermore, tests should be done using an open system where air is simply blown over the expos   surface of the insulation. With these tests, the turbulence level and scale in the free stream should be measured.

REFERENCES

ASHRAE (1989) **Fundamental Handbook**, S.I. edition. American Society of Heating, Refrigeration and Air Conditioning Engineers, Inc. Atlanta, GA.

Beavers, G.S and Joseph, D.D (1967), "Boundary Conditions at Naturally Permeable Wall", Journal of Fluid Mechanics, Vol. 30, pp. 197-210.

Bejan. P.G. (1984) ʃ   ctive Heat Ttransfer. Wiley- Interscience publications, John Wiley& Sors. New York, pp 343-380.

Berlad A.L., Tutu N., Yeh Y-J, Juang R., Krajewski R., Hope R., and Salzano F.J, (1980) "Air Intrusion Effects on the Performance of Permeable Insulation System. "Thermal Insulation Performance, ASTM STP 718, D.L McElroy and R.P.Tye,Eds., American Society for Testing and Materials, pp.191-194.

Chekhar. M.a.id Forest, T.W., (1995), "Effect of Air Flow on Heat Transfer in Porous Insulation". Proceeding of the 15th Canadian Congress of Applied Mechanics Victoria, B.C, May, pp. 476-477.

Chen, C.K , Hung, C.-I., and Cleaver, J.W. (1987), " Non-Darcian Effects on Vertical-Plate Transient Natural Convection in Porous Media with High-Porosities" Proceedings of the 1987 ASME-JSME Thermal joint conference. Vol.2, ASME, New York, NY., pp. 313-318.

Dale, J.D. and Ackerman, M.Y., (1993), " Evaluation of the Performance of Attic Turbine Ventilators". Proceedings of the 1993 Winter Meeting of ASHRAE Transaction: Research part 1, ASHRAE, Atlanta, GA. pp. 14-22.

Dybbs, A., Kar A., Groeneweg, M., Ling, J.X. and Maraghi, M., (1984) " A New Interpretation of Internal heat transfer Coefficients of Porous Media", ASME, Journal of Heat Ttransfer, New York, NY., pp. 1-7.

Forest, T.W., Nikel, K.G and Wilson, D.J (1993)" Moisture Deposition From Air Flow Through Wall Cavities." Proceedings Fourth international Symposium on Thermal Engineering & Science for Cold Region, US army Cold Regions Research and Engineering Laboratory, Hanover New Hampshire. Sept. pp.122-132.

Jackson, G.W and James, D.F. (1986), " The Permeability of Fibrous Media."The Canadian Journal of Chemical Engineering , Vol. 64, pp. 364-374.

Holman, J.P., (1963), Heat Transfer. McGraw-Hill Inc.N.Y. pg. 542.

Lapwood, E. R., (1948), " Convection of a fluid in porous medium, " Proc. Cambridge Philos. Soc. 44, 508.

Lundberg, R.E., McCuen, P .A., and Reynolds, W.C (1963), "Heat Transfer in Annular Passages. Hydrodynamically Developed Laminar Flow with arbitrarily Prescribed Wall Temperatures or Heat Fluxes. " Int. J. Heat Mass Transfer, Vol.6, pp 495-529.

McCuen, P.A., (1962) " Heat Transfer with Laminar and Turbulent Flow Between Parallel Planes with Constant and Variables Wall Temperature and Heat Flux." Stanford University Ph.D Thesis, Engineering Mechanics.

Muskat, M.(1937), The flow of Homogeneous Fluids Through Porous Media.McGraw-Hill book Company, Inc. N.Y. pp. 55-120.

Nikel, K.G (1993), " Moisture Deposition From Air flow Through Wall Cavities" M.Sc Thesis, Department of Mechanical Engineering, University of Alberta, Edmonton, Alberta.

Reynolds,W.C., Lundberg, R.E., and McCuen, P.A.(1963), "Heat Transfer in Annular Passages. General Formulation of the Problem for Arbitrarily Prescribed Wall Temperatures or Heat Fluxes. " Int. J. Heat Mass Transfer, Vol.6, pp. 483-494.

Saffman, P.J., (1971) " On the Boundary Condition at the Surface of a Porous Medium" Studies in Applied Mathematics. Vol. L No.2, Massachusetts Institute of Technology. Boston, MA. pp. 93-101.